Chapter 4

Castor oil-based nanofluids containing Al_2O_3, ZnO, GNP and MWCNT nano-additives

4.1: Preparation of Castor oil-based nanofluids containing Al_2O_3, ZnO, GNP and MWCNT nano-additives

Dispersing nano-additives in a base fluid needs special attention to develop an aggregate-free, stable liquid suspension without any deposition for a quite long period of time. The CO based nanofluid samples were prepared by combining nano-additives powder with pure CO by two step process. First, nano-additive was weighed using an analytical balance (Mettler Toledo XSR105) with a precision of ±0.02mg for preparing the nano-additive weight% of 0.05, 0.1, 0.2, and 0.5 at relevant quantity of CO. The nano-additive dispersed CO was sonicated using a high-power ultrasonication probe (Leela sonic) with a 500-watt output power and frequency of 20 kHz for 3 hours in pulse mode to get stable, homogeneous CO-based nanofluid containing nano-additives. Fig. 4.1 shows typical preparation of CO-based nanofluids containing different nano-additives. Fig. 4.2 to 4.6 displays the real image of nano-additives (Al_2O_3, ZnO, GNP and MWCNT) and it's nanofluids when dispersed with different concentration into CO base fluid. Moreover, the presence of an ester of ricinoleic acid in CO itself acts as a surfactant, which quite improves the stability of nano-dispersion [1, 2].

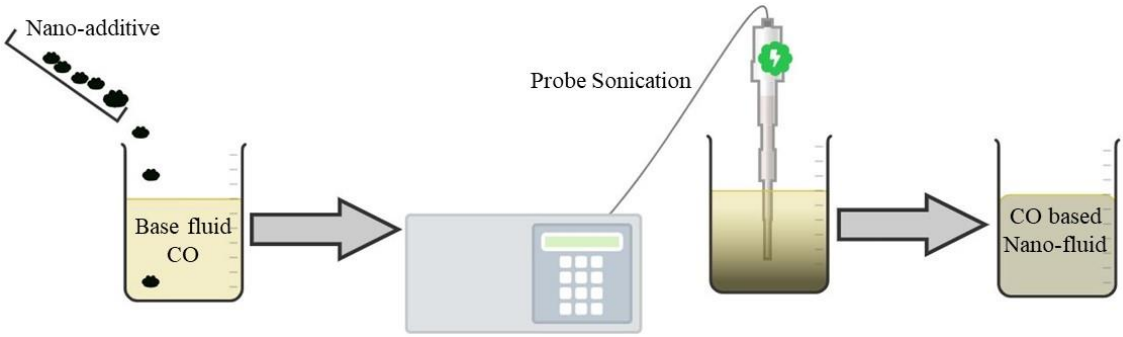

Fig. 4.1: Preparation of castor oil (CO)-based nanofluids containing nano-additives.

Following CO-based nanofluids prepared by dispersing nano-additives:

1. CO-based nanofluids containing Al_2O_3 nano-additives (**Al_2O_3/CO nanofluids**),
2. CO-based nanofluids containing ZnO nano-additives (**ZnO/CO nanofluids**),
3. CO-based nanofluids containing GNP nano-additives (**GNP/CO nanofluids**), and
4. CO-based nanofluids containing MWCNT nano-additives (**MWCNT/CO nanofluids**)

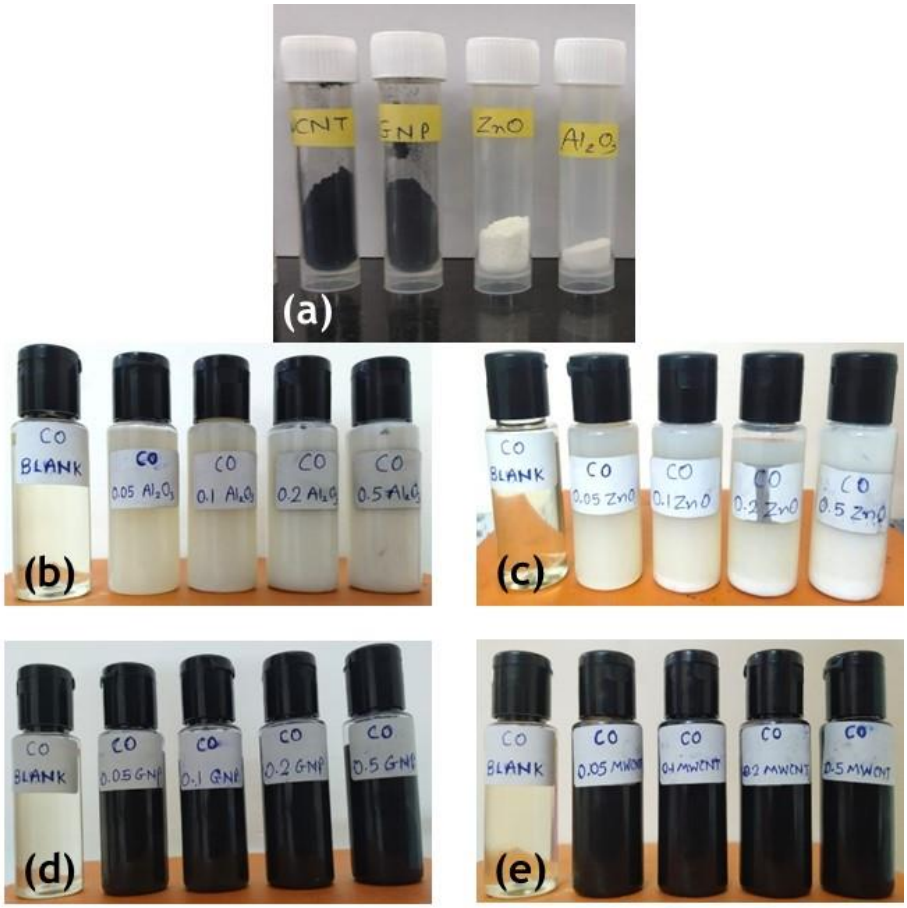

Fig. 4.2: **(a)** Nano-additives (Al_2O_3, ZnO, GNP and MWCNT) used to prepare CO-based nanofluids, **(b)** Al_2O_3/CO nanofluids with different Al_2O_3 concentrations, **(c)** ZnO/CO nanofluids with different ZnO concentrations, **(d)** GNP/CO nanofluids with different GNP concentrations, and **(e)** MWCNT/CO nanofluids with different MWCNT concentrations.

4.2: CO-based nanofluids containing Al_2O_3 nano-additives (Al_2O_3/CO nanofluids)

In this study, a comprehensive rheological investigation was conducted to evaluate dynamic viscosity of both pure CO and Al_2O_3/CO nanofluids under different Al_2O_3 concentrations, shear rates, and temperature conditions. The main focus was to understand the influence of Al_2O_3 weight % and temperature on the dynamic viscosity and thermal conductivity of Al_2O_3/CO nanofluids. The obtained results shed light on the potential uses of Al_2O_3/CO nanofluids as lubricating oils.

4.2.1: Flow characteristics of Al_2O_3/CO nanofluids using rheometry

Fig. 4.3 exhibits the impact of shear rate on the dynamic viscosity of Al_2O_3/CO nanofluids at different Al_2O_3 weight % and temperatures ranging from 40ºC to 100ºC. The findings indicated that the dynamic viscosity of both Al_2O_3/CO nanofluids and pure CO decreases linearly with increasing shear rates at 40ºC for all Al_2O_3 concentrations. This shows shear thinning behaviour of non-Newtonian fluid. At higher shear rates and higher temperatures i.e., 60ºC, 80ºC, and 100ºC, all nano-fluids exhibit linear behaviour indicating Newtonian fluid characteristic i.e., fluids have a constant viscosity regardless of the shear rates applied. The experimental findings suggest a Newtonian fluid behaviour for both Al_2O_3/CO nanofluids and pure CO at higher shear rates and higher temperature within the experimental range. Furthermore, at higher shear rates and temperatures, nanofluids with higher Al_2O_3 weight % exhibit a slight shear-thinning behaviour compared to nanofluids with lower Al_2O_3 weight%. This finding indicates raised Al_2O_3 concentration, represented by weight %, has a notable impact on enhancing shear thinning in the Al_2O_3/CO nanofluids.

Fig. 4.4 presents the impact of Al_2O_3 weight % on the dynamic viscosity of constantly-temperatured nanofluids. The Al_2O_3 concentration has a significant influence on dynamic viscosity within the shear rate range of 100 to 5000 s^{-1}. At 40ºC dynamic viscosity of all nanofluids increases with enhancing Al_2O_3 concentration. However, rate of increase in dynamic viscosity with increasing Al_2O_3 nano-additive concentration became very less at all shear rates except 100 s^{-1}. Increased dynamic viscosity of nanofluids attributed to the increased flow resistance depicted by solid Al_2O_3 nanoparticles in CO fluid. Consequently, increasing the Al_2O_3 concentration results in higher nanofluid

viscosity. However, it's important to note that the dynamic viscosity does not always increase significantly with concentration. For instance, in Fig. 4.4 (c) and 6(d), the increase in dynamic viscosity is relatively low compared to lower temperature of 40ºC.

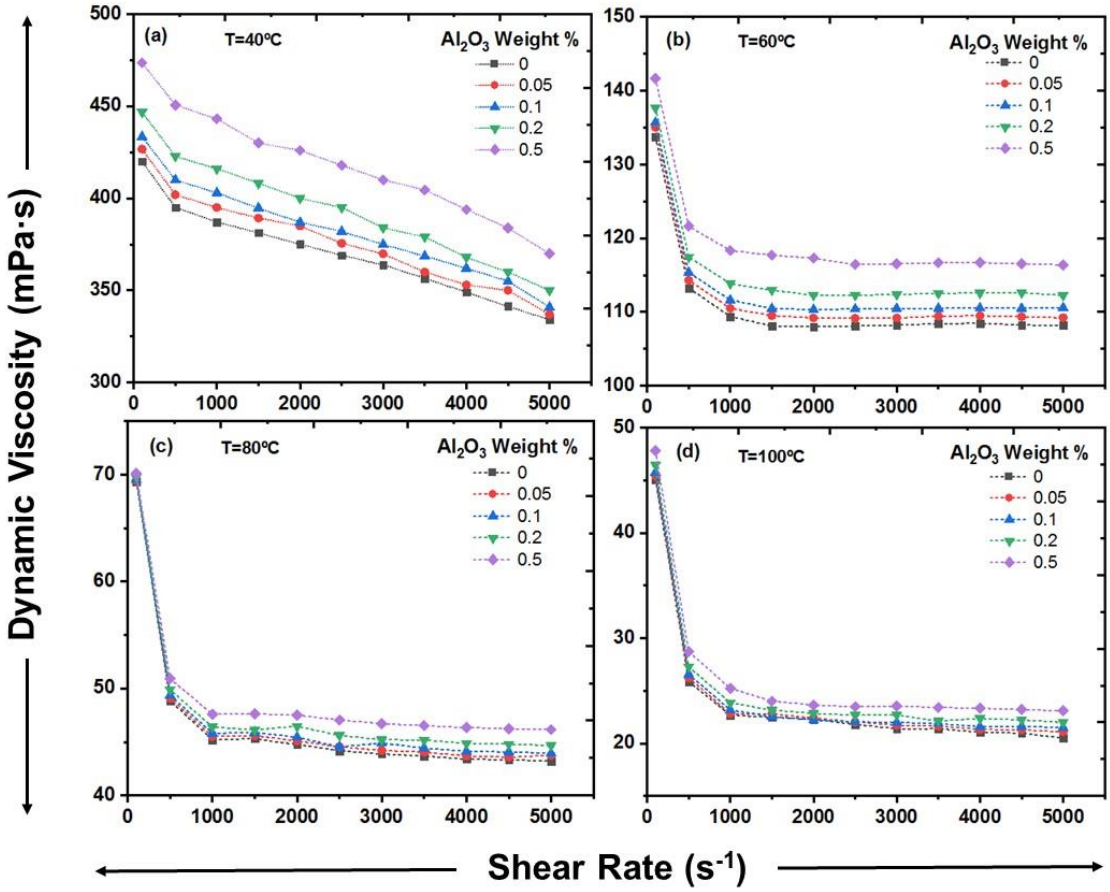

Fig. 4.3 (a-d): Effect of shear rate on dynamic viscosity of Al_2O_3/CO nanofluids at different mass fraction.

Fig. 4.5 depicts the influence of temperature on the dynamic viscosity of pure CO and Al_2O_3/CO nanofluids with varying nano-additive Al_2O_3 weight %. This analysis is conducted at constant shear rates of 500 s^{-1} and 5000 s^{-1}. As the temperature rises from 40°C to 100°C, the dynamic viscosity drops for CO fluids and Al_2O_3/CO nanofluids. For instance, at a shear rate of 500 s^{-1}, the Al_2O_3/CO nanofluid with a 0.5 weight% Al_2O_3 concentration shows a viscosity of 370 mPa at 40°C, which decreases to 23 mPa at 100°C. Similar trends are observed for other nano-additive Al_2O_3 weight %. These observations can be attributed to a decreased intermolecular adhesion force as temperature rises. Moreover, the effect of solid nano-additive Al_2O_3 concentration on dynamic viscosity is more prominent at lower temperatures. However, this impact starts to diminish as the temperature increases.

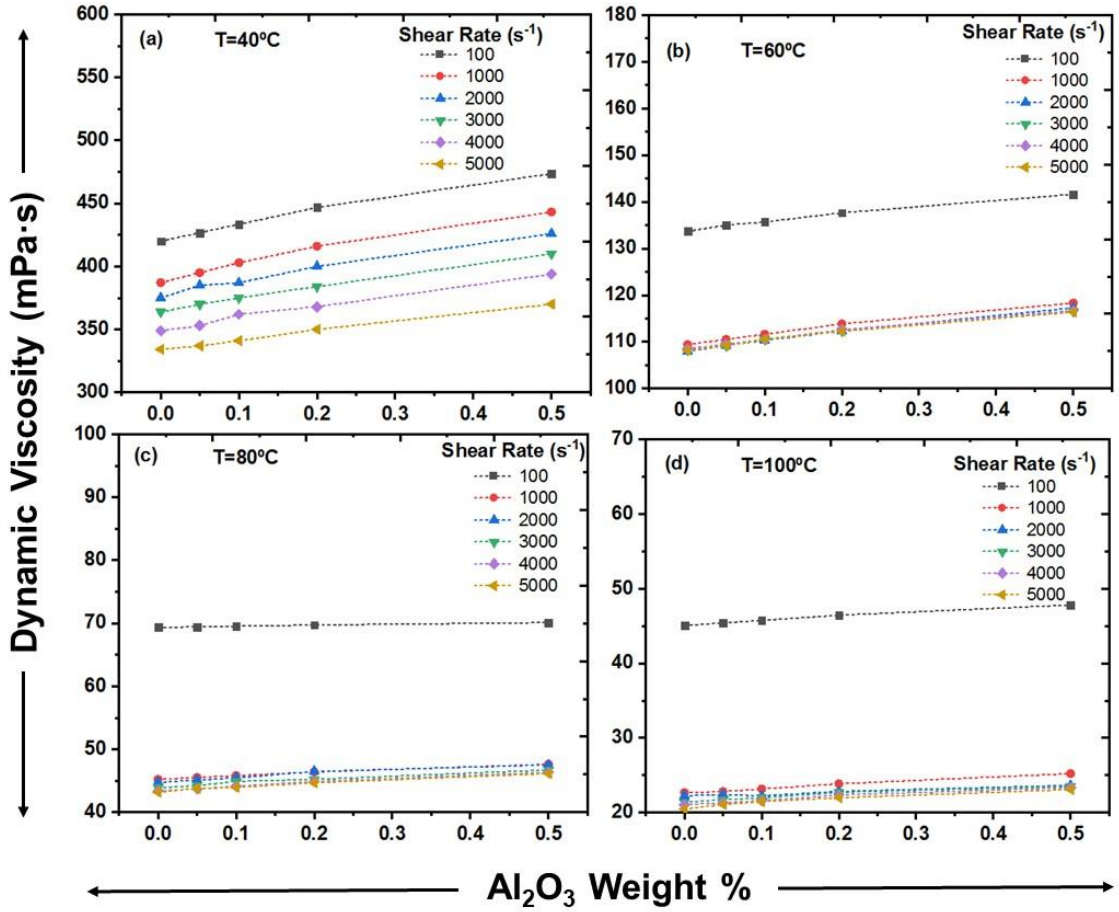

Fig. 4.4 (a-d): Effect of solid mass fractions on dynamic viscosity of Al_2O_3/CO nanofluids at different shear rates.

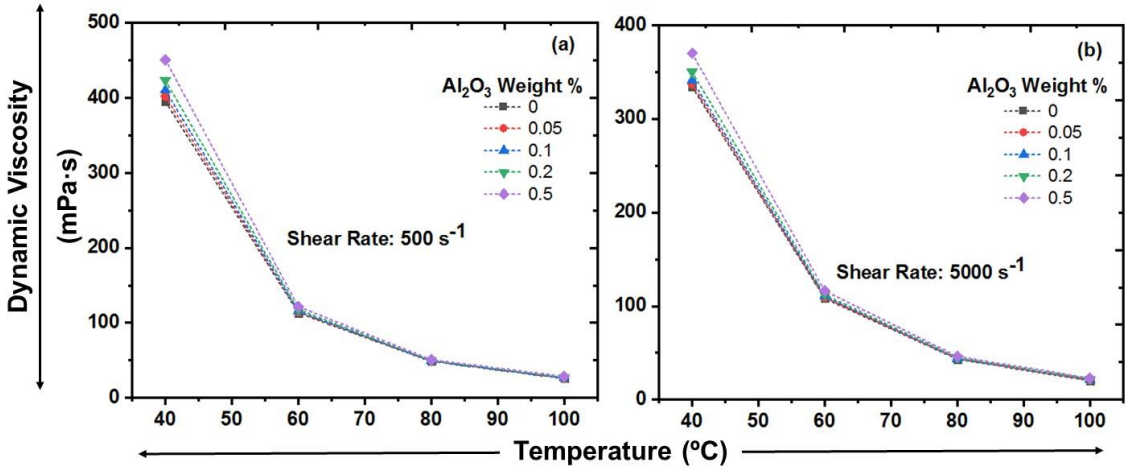

Fig. 4.5 (a-b): Effect of temperature on the dynamic viscosity of Al_2O_3/CO nanofluids at different solid mass fractions.

In Fig. 4.6 (a-d), the correlation between shear rate & shear stress of Al_2O_3/CO nanofluid is depicted at different temperatures for various Al_2O_3 weight % (0.0, 0.05, 0.1, 0.2, and 0.5). The figures demonstrate that shear stress increases as shear rate increases

across all temperatures. To determine the flow behaviour of the fluid, whether it follows Newtonian flow or non-Newtonian flow, the Ostwald-de-Waele (OdW) model is employed using Equation (1) as discussed in the chapter 1 [3-5]. In this analysis, fitting of power law curves was applied to the shear stress vs. shear rate curve to find the values of consistency index (m) and power law index (n). The obtained values of m and n are displayed in Table 4.1.

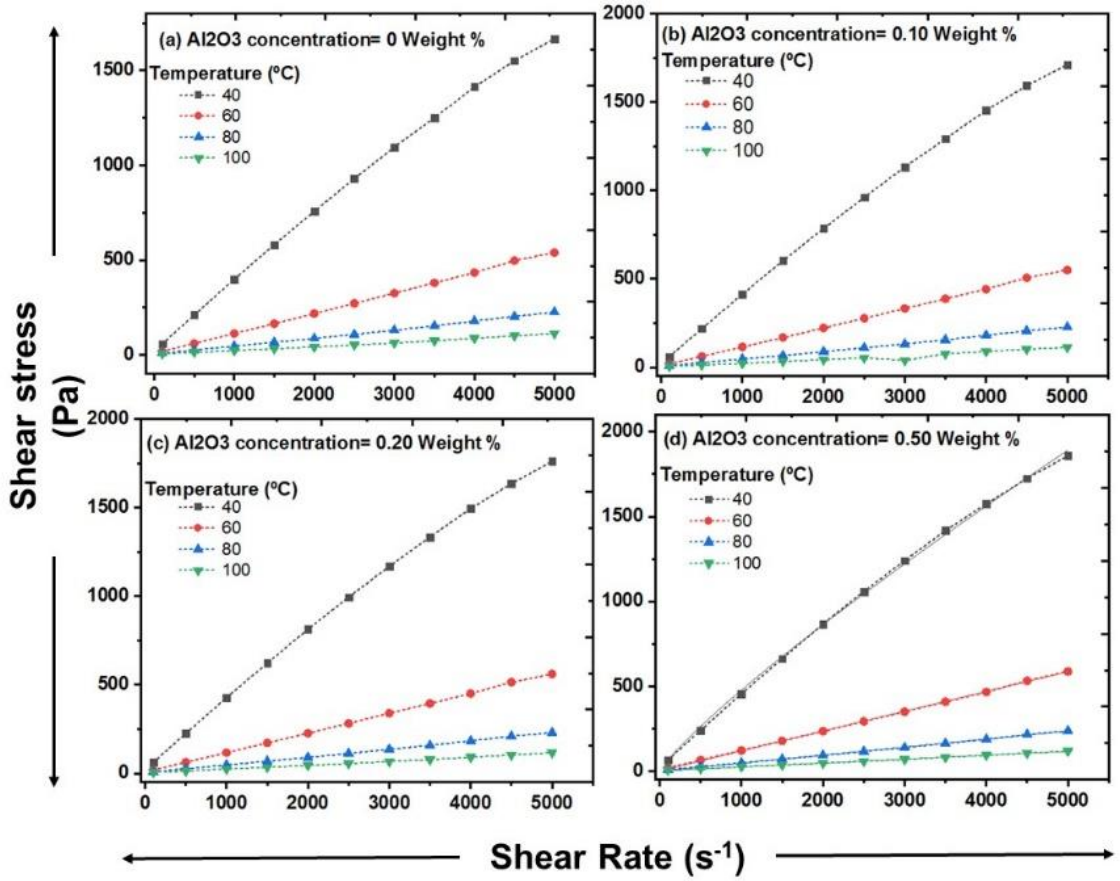

Fig. 4.6 (a-d): Shear stress vs. shear rate at various temperature for Al_2O_3/CO nanofluids.

As displayed in Fig. 4.7, power law index (n) values are less than one at 40°C for all nano-additive Al_2O_3 weight % and temperature ranges of the nanofluids, indicating a pseudo plastic non-Newtonian fluid flow behaviour. The values of n for all nano-additive Al_2O_3 weight % and temperatures (60°C and 80°C) of the nanofluids are close to or equal to one, indicating a Newtonian flow behaviour. At 100°C with increasing Al_2O_3 concertation in CO, different flow characteristics are observed. At lower concentration up to 0.1 weight %, CO and Al_2O_3/CO nanofluids show dilatant fluid non-Newtonian fluid behaviour. At 0.2 weight %, Al_2O_3/CO nanofluid show Newtonian fluid behaviour. While,

at 0.5 weight %, Al_2O_3/CO nanofluid show pseudo plastic non-Newtonian fluid flow behaviour. This observation suggests that at higher temperature of 100°C, Al_2O_3/CO nanofluids shows different flow behaviours depending on nano-additive Al_2O_3. This may help in designing the Al_2O_3/CO nanofluid as per flow behaviour requirement in different industrial applications.

Table 4.1: The power law index (n) and consistency index (m) values of Al_2O_3/CO nano-fluids.

Temperature (°C)	Indexes	Al_2O_3 concentration (Weight %)				
		0	**0.05**	**0.1**	**0.2**	**0.5**
40	m	959	999	1054	1135	1294
	n	0.8780	0.8749	0.8701	0.8646	0.8556
60	m	123	124	127	131	129
	n	0.9850	0.9859	0.9837	0.9826	0.9885
80	m	40	44	40	45	46
	n	1.0125	1.0021	1.0148	1.0016	1.0044
100	m	17	8	9	22	32
	n	1.0349	1.022	1.0026	1.0032	0.9640

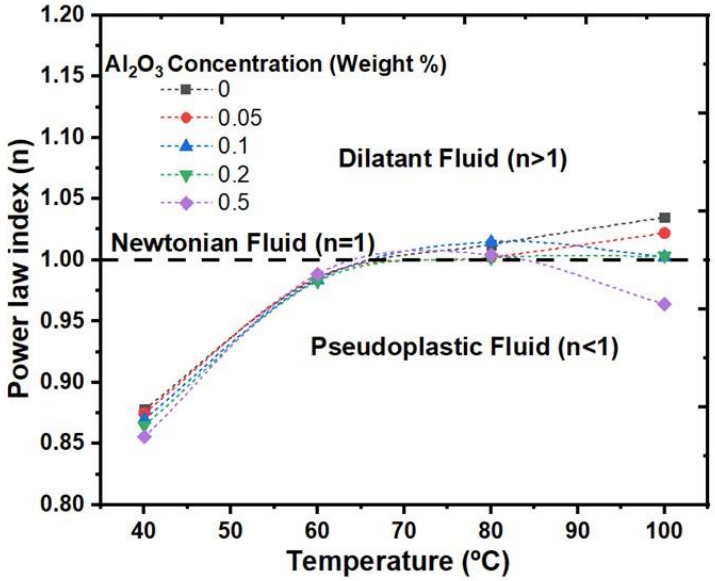

Fig. 4.7: Power law index for different solid mass fractions and temperature for Al_2O_3/CO nanofluids.

Furthermore, Fig. 4.8 depicts the relationship between the nanofluids' temperature & the consistency index (m) for different Al_2O_3 concentrations. The findings clearly demonstrate m value declines with increasing temperature. This indicates, as temperature rises, the fluid's mobility decreases, resulting in reduced flow resistance. It is noteworthy that the consistency index does not change much with the Al_2O_3 concentration at higher

temperatures. This observation confirms that higher Al_2O_3 concentrations in the base fluid do not substantially increase resistance to fluid flow.

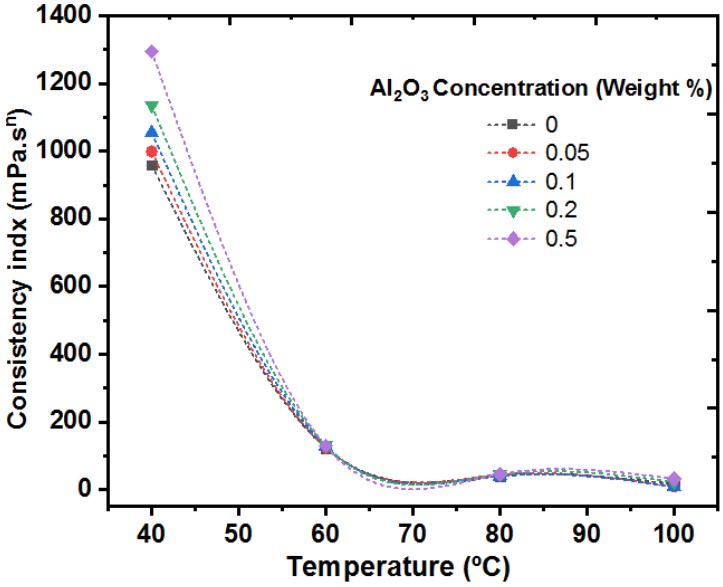

Fig. 4.8: Consistency index for different solid mass fractions and temperatures for Al_2O_3/CO nanofluids.

4.2.2: Thermal conductivity characteristics of Al_2O_3/CO nanofluids

In Fig. 4.9 (a), the thermal conductivity of pure CO and Al_2O_3/CO nanofluid is shown for Al_2O_3 concentration over a temperature: 30°C to 70°C. The data reveal that thermal conductivity increases as increasing the Al_2O_3 concentration. Moreover, at higher Al_2O_3 concentrations, thermal conductivity exhibits a steeper slope, indicating a more pronounced enhancement. This increased thermal conductivity is attributed to the higher heat conductivity of Al_2O_3 which better incorporated into the CO fluid. It is noteworthy to notice, thermal conductivity of both CO fluid and the Al_2O_3/CO nanofluid with a 0.05 weight % Al_2O_3 concentration diminish as temperature increases. However, a reversal in thermal conductivity behaviour is observed at a Al_2O_3 concentration above 0.1 weight % in the BO. In this case, the thermal conductivity of Al_2O_3/CO nanofluids increases with enhancing temperature. This is explained by the increased interaction and quite homogeneous dispersion of Al_2O_3 within the CO fluid at higher temperatures. These changes are driven by the energy transfer between the layers of the nanofluid, resulting in enhanced heat transfer capabilities of the nanofluids [6-8]. Overall, the findings show that Al_2O_3/CO nanofluids have enhanced thermal conductivity relative to the pure CO fluid.

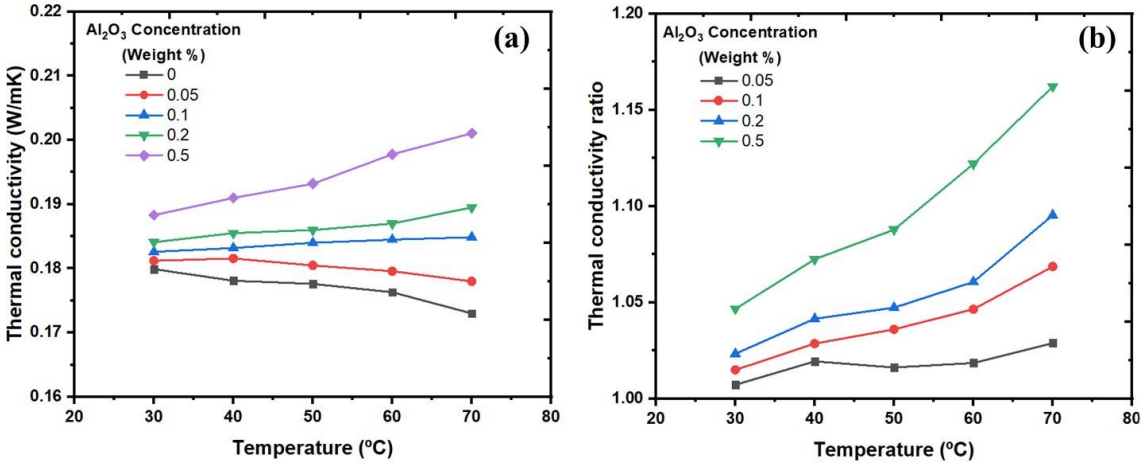

Fig. 4.9: (a) Thermal conductivity of Al_2O_3/CO nanofluids, and (b) thermal conductivity ratio of Al_2O_3/CO nanofluids.

The thermal conductivity ratio of the Al_2O_3/CO nanofluid relative to the CO base fluid is shown in Fig. 4.9 (b). The ratio increases with enhancing temperature. At low Al_2O_3 weight %, there are minimal increases in thermal conductivity because of the lower concentration of Al_2O_3 in the fluid. However, as the Al_2O_3 concentration increases, the number of nanoparticles & their collisions also increases, resulting in effective heat transfer between the fluid layers [9, 10]. This results in greater thermal conductivity values for the Al_2O_3/CO nanofluid relative to the base CO fluid. In our study, the thermal conductivity of the Al_2O_3/CO nanofluid increased by 16.2% at 70°C for a Al_2O_3 concentration of 0.5 weight%. This significant enhancement demonstrates the capability of Al_2O_3/CO nanofluids to enhance heat transfer performance in various industrial applications.

4.3: CO-based nanofluids containing ZnO nano-additives (ZnO/CO nanofluids)

In this study, a comprehensive rheological investigation was carried out to assess the dynamic viscosity of both pure CO and ZnO/CO nanofluids under different ZnO concentrations, shear rates, and temperature conditions. The main focus was to understand the influence of ZnO weight % and temperature on the dynamic viscosity and thermal conductivity of ZnO/CO nanofluids. The obtained results shed light on the potential uses of ZnO/CO nanofluids as lubricating oils.

4.3.1: Flow characteristics of ZnO/CO nanofluids using rheometry

Fig. 4.10 exhibits the impact of shear rate on the dynamic viscosity of ZnO/CO nanofluids at different ZnO weight % and temperature: 40ºC to 100ºC. The findings indicated that the dynamic viscosity of both ZnO/CO nanofluids and pure CO decreases linearly with increasing shear rates at 40ºC for all nano-additive concentrations. This shows shear thinning behaviour of non-Newtonian fluid. At higher shear rates and higher temperatures i.e., 60ºC, 80ºC, and 100ºC, all fluids exhibit linear behaviour indicating Newtonian fluid characteristic i.e., fluids have a constant viscosity regardless of the shear rates applied. The experimental findings suggest a Newtonian fluid behaviour for both ZnO/CO nanofluids and pure CO at higher shear rates and higher temperature within the experimental range. Furthermore, at higher shear rates and higher temperature, nanofluids with higher ZnO weight % exhibit a slight shear-thinning behaviour compared to nanofluids with lower ZnO weight %. This observation suggests that increased ZnO concentration, represented by weight %, has a notable impact on enhancing shear thinning in both ZnO/CO nanofluids and pure CO.

Fig. 4.11 presents the effect of ZnO weight% on dynamic viscosity of constantly-temperatured nanofluids. The ZnO concentration has a significant influence on the dynamic viscosity within the shear rate range of 100 to 5000 s^{-1}. At 40ºC dynamic viscosity of all nanofluids increases with enhancing ZnO nano-additive concentration. However, rate of increase in dynamic viscosity with increasing ZnO nano-additive concentration became very less at all shear rates except 100 s^{-1}. Increased dynamic viscosity of nanofluids attributed to the increased flow resistancedepicted by the presence of solid ZnO nano-additive in the CO fluid. Consequently, increasing the ZnO nano-

additive concentration results in higher nanofluid viscosity. However, it's important to note that the dynamic viscosity does not always increase significantly with concentration. For instance, in Fig. 4.11 (c) and 6(d), the increase in dynamic viscosity is relatively low compared to lower temperature of 40ºC.

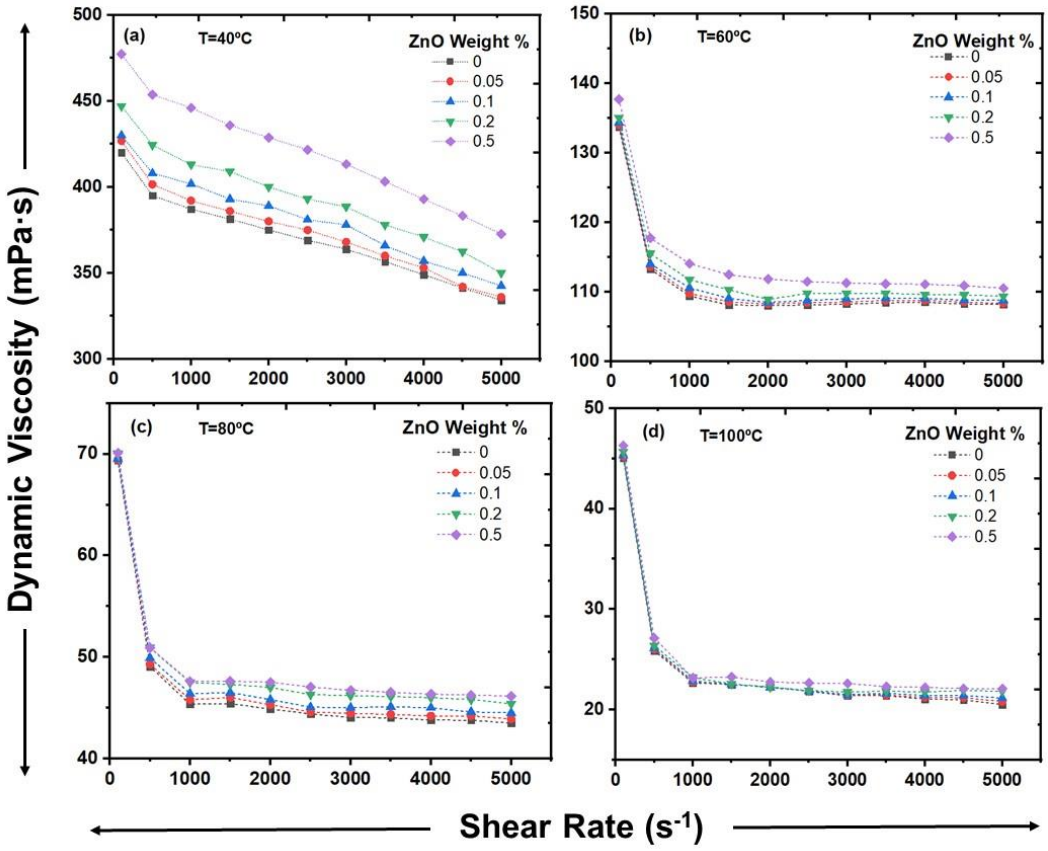

Fig. 4.10 (a-d): Effect of shear rate on dynamic viscosity of ZnO/CO nanofluids at different mass fraction.

Fig. 4.12 depicts the effect of temperature on the dynamic viscosity of pure CO and ZnO/CO nanofluids with varying ZnO weight %. This analysis is conducted at constant shear rates of 500 s^{-1} and 5000 s^{-1}. As the temperature rises from 40°C to 100°C, the dynamic viscosity drops for CO fluids and ZnO/CO nanofluids. For instance, at a shear rate of 5000 s^{-1}, the ZnO/CO nanofluid with a 0.5 weight% ZnO concentration shows a viscosity of 373 mPa at 40°C, which decreases to 24 mPa at 100°C. Similar trends are observed for other nano-additive ZnO weight %. These observations can be attributed to a decreased intermolecular adhesion force as temperature rises. Moreover, the effect of solid nano-additive ZnO concentration on dynamic viscosity is more prominent at lower temperatures. However, results shows that this impact starts to diminish as the temperature increases.

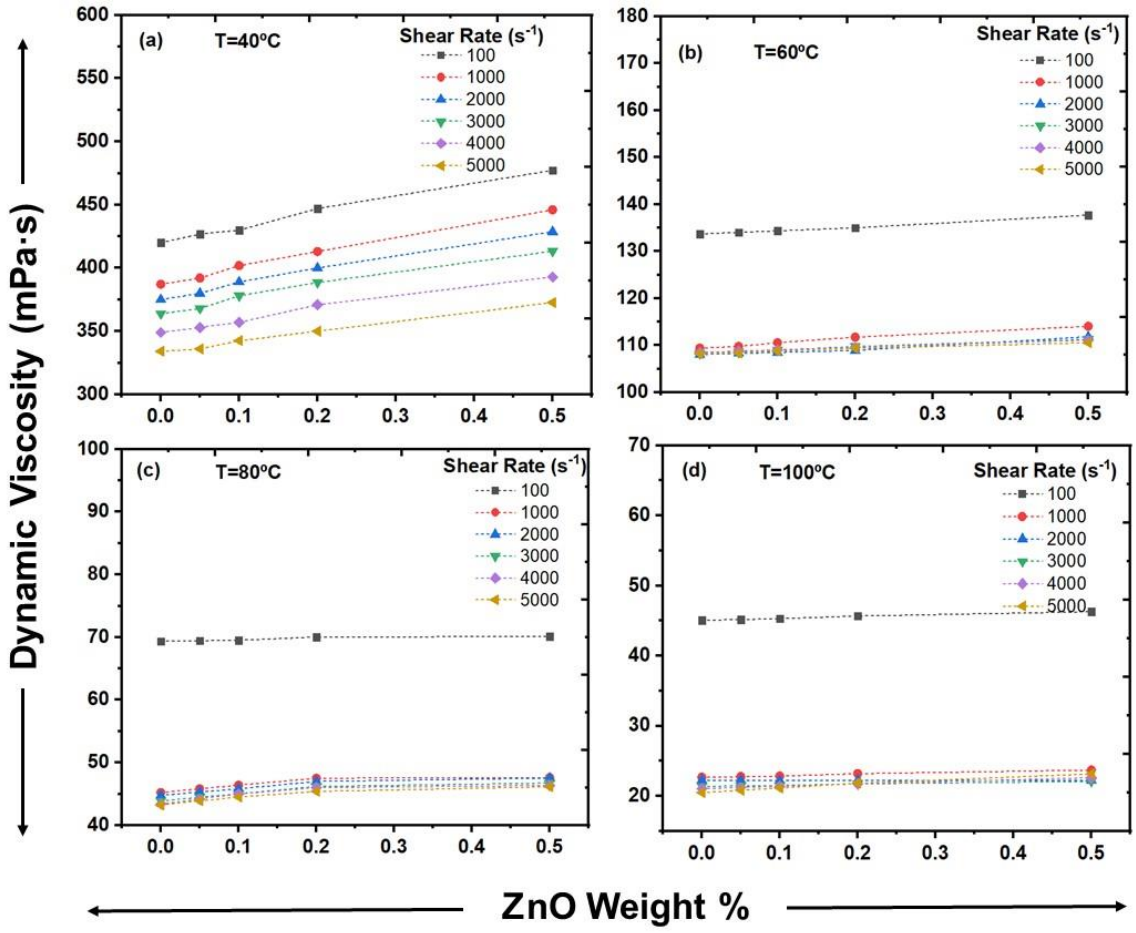

Fig. 4.11 (a-d): Effect of solid mass fractions on dynamic viscosity of ZnO/CO nanofluids at different shear rates.

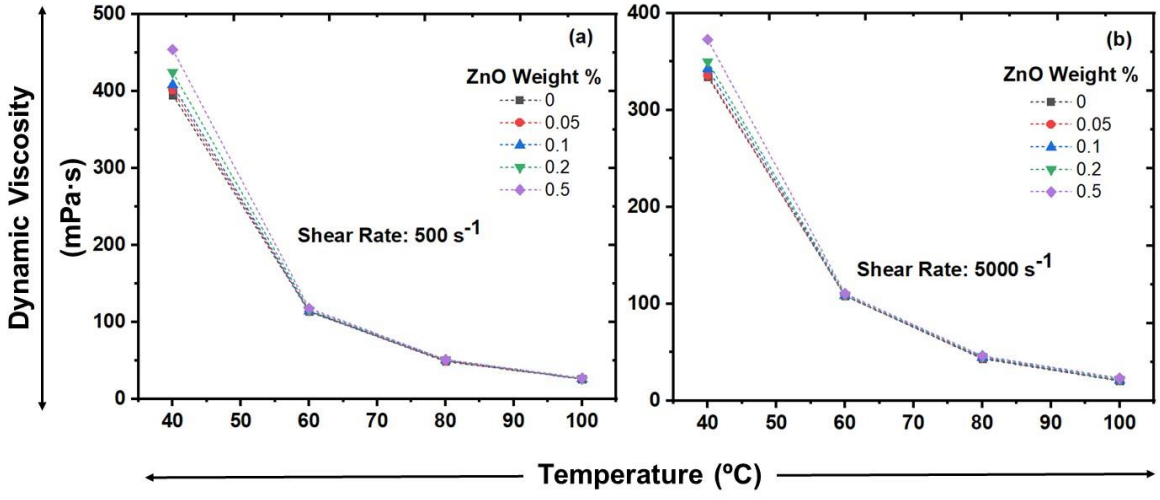

Fig. 4.12 (a-b): Effect of temperature on the dynamic viscosity of ZnO/CO nanofluids at different solid mass fractions.

In Fig. 4.13 (a-d), the correlation between shear rate & shear stress of ZnO/CO nanofluid is depicted at different temperatures for various ZnO weight % (0.0, 0.05, 0.1, 0.2, and 0.5). The figures demonstrate that shear stress increases as shear rate increases across all temperatures. To determine the flow behaviour of the fluid, whether it follows Newtonian flow or non-Newtonian flow, the Ostwald-de-Waele (OdW) model is employed using Equation (1) as discussed in introduction part of chapter 1 [3-5]. In this analysis, fitting of power law curves was applied to the shear stress vs. shear rate curve to calculate the values of consistency index (m) and power law index (n). The obtained values of m and n are displayed in Table 4.2.

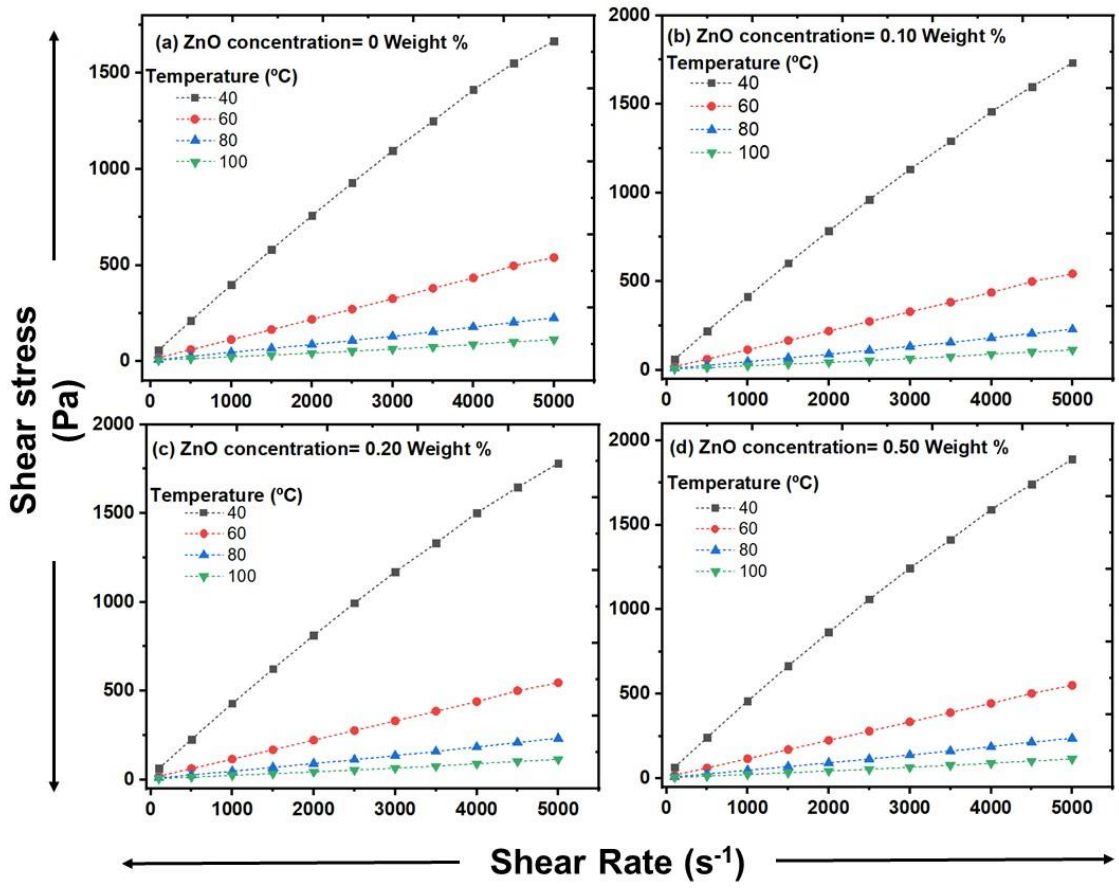

Fig. 4.13 (a-d): Shear stress vs. shear rate at various temperature for ZnO/CO nanofluids.

As demonstrated in Fig. 4.14, power law index (n) values are less than one at 40°C for all nano-additive ZnO weight % and temperature ranges of the nanofluids, indicating a pseudo plastic non-Newtonian fluid flow behaviour. The values of n for all nano-additive ZnO weight % and temperature (60°C) of the nanofluids are close to or equal to one, indicating a mild Newtonian fluid flow behaviour. However, at 80°C with increasing nano-

additive ZnO concertation in CO, pure Newtonian fluid flow behaviour is observed. For 100°C temperature, at lower concentration up to 0.2 weight %, CO and ZnO/CO nanofluids show dilatant fluid non-Newtonian fluid behaviour. While, at 0.5 weight %, ZnO/CO nanofluid show complete Newtonian fluid flow behaviour. This observation suggests that at higher temperature of 100°C, ZnO/CO nanofluids shows different flow behaviours depending on nano-additive ZnO. This may help in designing the ZnO/CO nanofluid as per flow behaviour requirement in different industrial applications.

Table 4.2: The power law index (n) and consistency index (m) values of ZnO/CO nano-fluids.

Temperature (°C)	Indexes	ZnO concentration (Weight %)				
		0	**0.05**	**0.1**	**0.2**	**0.5**
40	m	959	997	987	1064	1195
	n	0.8780	0.8752	0.8787	0.8731	0.8663
60	m	123	127	128	133	144
	n	0.9850	0.9816	0.9810	0.9767	0.9686
80	m	40	41	41	41	44
	n	1.0125	1.0103	1.0126	1.0122	1.0071
100	m	17	18	18	19	23
	n	1.0349	1.0267	1.0257	1.0169	0.9986

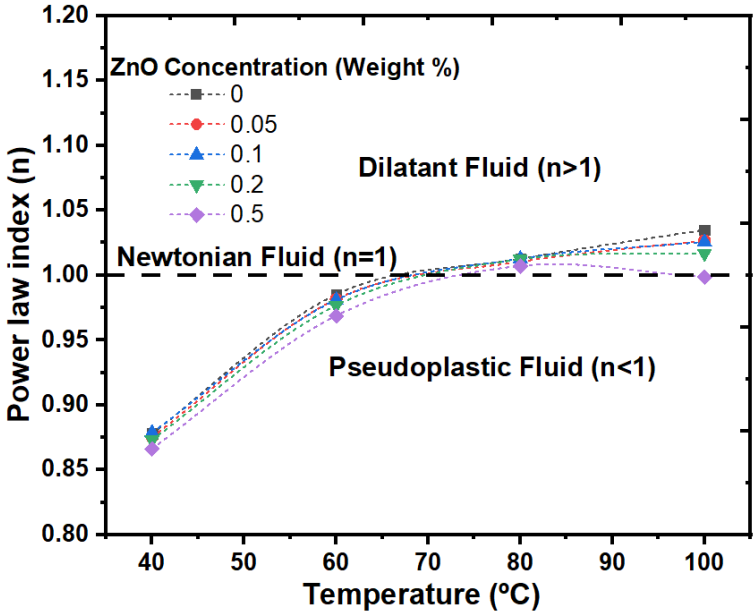

Fig. 4.14: Power law index for different solid mass fractions and temperature for ZnO/CO nanofluids.

Furthermore, Fig. 4.15 depicts the relationship between the nanofluids' temperature & the consistency index (m) for different ZnO weight concentrations. The results clearly demonstrate m value declines with increasing temperature. This indicates, as temperature

rises, the fluid's mobility decreases, resulting in reduced flow resistance. It is noteworthy that the consistency index does not change much with the ZnO concentration at higher temperatures. This observation confirms that higher ZnO concentrations in the base fluid do not substantially increase resistance to fluid flow.

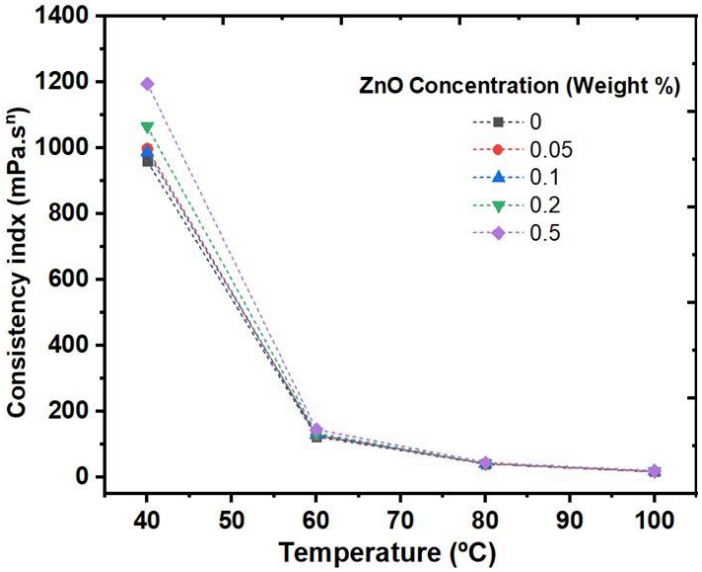

Fig. 4.15: Consistency index for different solid mass fractions and temperatures for ZnO/CO nanofluids.

4.3.2: Thermal conductivity characteristics of ZnO/CO nanofluids

In Fig. 4.16 (a), the thermal conductivity of pure CO and ZnO/CO nanofluid is shown for ZnO concentration over a temperature: 30°C to 70°C. The data reveal that thermal conductivity increases as increasing the ZnO concentration. Moreover, at higher ZnO concentrations, the thermal conductivity exhibits a steeper slope, indicating a more pronounced enhancement. This increase in thermal conductivity is attributed to the higher heat conductivity of ZnO incorporated into the CO fluid. It is noteworthy to notice, thermal conductivity of both CO fluid and the ZnO/CO nanofluid with a 0.05 weight % ZnO concentration diminish as temperature increases. However, a reversal in thermal conductivity behaviour is observed at a ZnO concentration above 0.1 weight % in the BO. In this case, the thermal conductivity of ZnO/CO nanofluids increases with enhancing temperature. This is explained by the increased interaction and spread of ZnO within the CO fluid at higher temperatures. These changes are driven by the energy transfer between the layers of the nanofluid, resulting in enhanced heat transfer capabilities of the nanofluids [6-8]. Overall, the findings show that ZnO/CO nanofluids have enhanced thermal conductivity relative to the pure CO fluid.

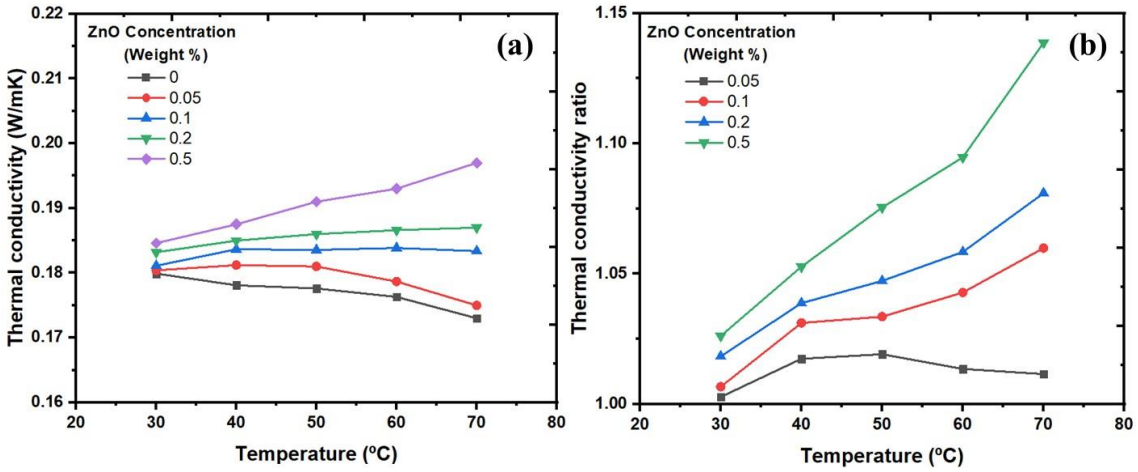

Fig. 4.16: (a) Thermal conductivity of ZnO/CO nanofluids, and (b) thermal conductivity ratio of ZnO/CO nanofluids.

The thermal conductivity ratio of the ZnO/CO nanofluid relative to the CO base fluid is shown in Fig. 4.16 (b). The ratio increases with enhancing temperature. At low ZnO weight %, there are minimal increases in thermal conductivity because of the lower concentration of ZnO in the fluid. However, as the ZnO concentration increases, the number of nanoparticles & their collisions also increases, resulting in effective heat transfer between the fluid layers [9, 10]. This results in greater thermal conductivity values for the ZnO/CO nanofluid relative to the base CO fluid. In our study, the thermal conductivity of the ZnO/CO nanofluid increased by 13.9% at 70°C for a ZnO weight % of 0.5%. This moderate enhancement demonstrates that of ZnO/CO nanofluids have less potential use for heat transfer in various applications.

4.4: CO-based nanofluids containing GNP nano-additives (GNP/CO nanofluids)

In this study, a comprehensive rheological investigation was carried out to assess the dynamic viscosity of both pure CO and GNP/CO nanofluids under different GNP concentrations, shear rates, and temperature conditions. The main focus was to understand the influence of GNP weight % and temperature on the dynamic viscosity and thermal conductivity of GNP/CO nanofluids. The obtained results shed light on the potential uses of GNP/CO nanofluids as lubricating oils.

4.4.1: Flow characteristics of GNP/CO nanofluids using rheometry

Fig. 4.17 exhibits the impact of shear rate on the dynamic viscosity of GNP/CO nanofluids at different GNP weight % and temperatures ranging from 40ºC to 100ºC. The findings indicated that the dynamic viscosity of both GNP/CO nanofluids and pure CO decreases linearly with increasing shear rates at 40ºC for all nano-additive concentrations. Notable observation found that at 40ºC temperature, as shear rate increases to maximum, all GNP/CO nanofluids exhibit nearly same dynamic viscosity indicating GNP nano-additive has not altered fluid characteristic at 40 ºC and high shear rate condition. At higher shear rates and higher temperatures i.e., 60ºC, 80ºC, and 100ºC, all fluids exhibit linear behaviour indicating Newtonian fluid characteristic i.e., fluids have a constant viscosity regardless of the shear rates applied. The experimental findings suggest a Newtonian fluid behaviour for both GNP/CO nanofluids and pure CO at higher shear rates and higher temperature within the experimental range. Furthermore, at higher shear rates and higher temperature, nanofluids with lower GNP weight % exhibit a slight shear-thinning behaviour compared to nanofluids with higher GNP weight %. This observation suggests that increased GNP concentration, represented by weight %, has a notable impact on maintaining Newtonian fluid behaviour in both GNP/CO nanofluids and pure CO.

Fig. 4.18 presents the effect of GNP weight % on the dynamic viscosity of constantly-temperatured nanofluids. The GNP concentration has a significant influence on the dynamic viscosity within the shear rate range of 100 to 5000 s^{-1}. At 40ºC dynamic viscosity of all nanofluids increases marginally with increasing GNP nano-additive concentration. However, rate of increase in dynamic viscosity with increasing GNP nano-additive concentration became very less at all shear rates except 100 s^{-1}. Increased dynamic

viscosity of nanofluids attributed to the increased flow resistancedepicted by the presence of solid GNP nano-additive in the CO fluid. Consequently, increasing the GNP nano-additive concentration results in higher nanofluid viscosity. However, it's important to note that the dynamic viscosity does not always increase significantly with concentration. For instance, in Fig. 4.18 (c) and 6(d), the increase in dynamic viscosity is relatively low compared to lower temperature of 40ºC.

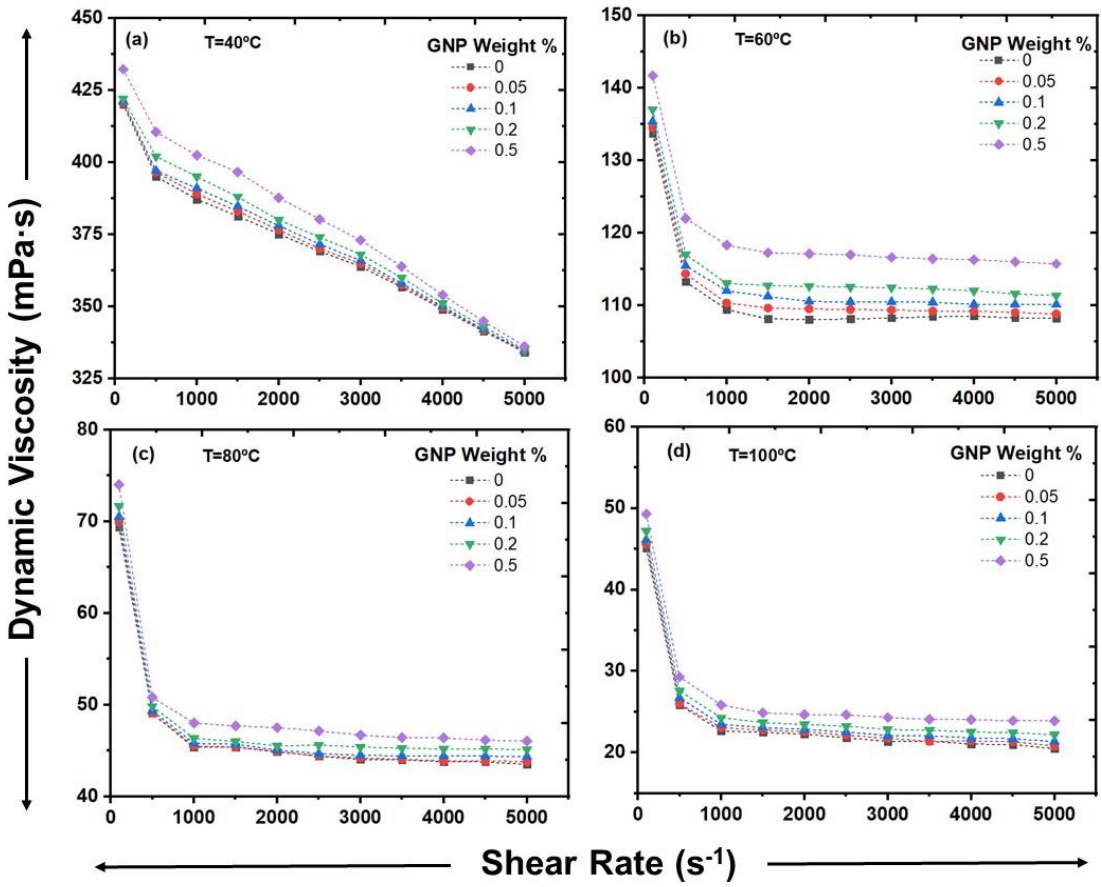

Fig. 4.17 (a-d): Effect of shear rate on dynamic viscosity of GNP/CO nanofluids at different mass fraction.

Fig. 4.19 depicts the influence of temperature on the dynamic viscosity of pure CO and GNP/CO nanofluids with varying nano-additive GNP weight %. This analysis is conducted at constant shear rates of 500 s^{-1} and 5000 s^{-1}. As the temperature rises from 40°C to 100°C, the dynamic viscosity drops for CO fluids and GNP/CO nanofluids. For instance, at a shear rate of 500 s^{-1}, the GNP/CO nanofluid with a 0.5 weight% GNP concentration shows a viscosity of 410 mPa at 40°C, which decreases to 29 mPa at 100°C. Similar trends are observed for other nano-additive GNP weight %. These observations can be attributed to a decreased intermolecular adhesion force as temperature rises. Moreover,

the effect of solid nano-additive GNP concentration on dynamic viscosity is more prominent at lower temperatures. However, this impact starts to diminish as the temperature increases.

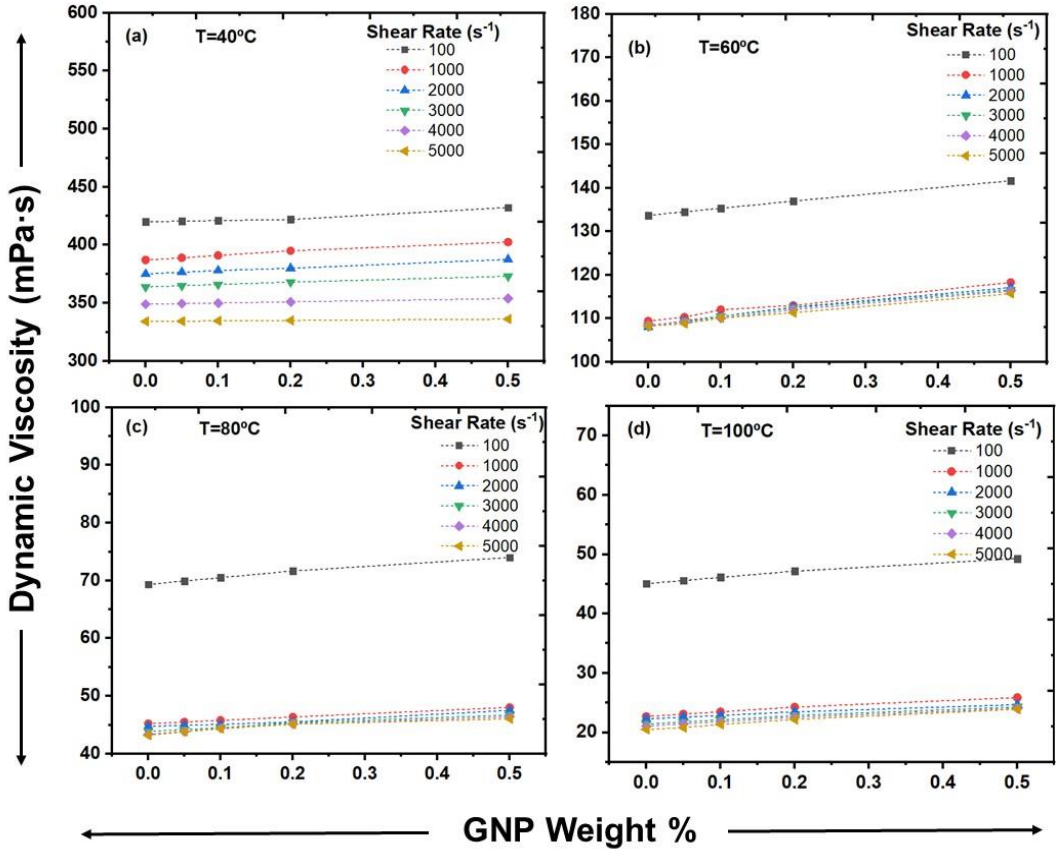

Fig. 4.18 (a-d): Effect of solid mass fractions on dynamic viscosity of GNP/CO nanofluids at different shear rates.

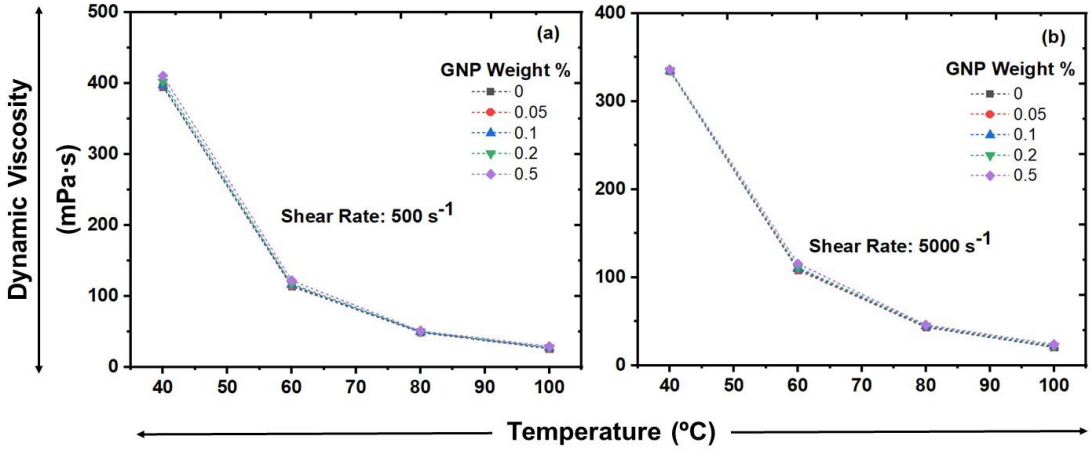

Fig. 4.19 (a-b): Effect of temperature on the dynamic viscosity of GNP/CO nanofluids at different solid mass fractions.

In Fig. 4.20 (a-d), the correlation between shear rate & shear stress of GNP/CO nanofluid is depicted at different temperatures for various GNP weight % (0.0, 0.05, 0.1,

0.2, and 0.5). The figures demonstrate that shear stress increases as shear rate increases across all temperatures. To determine the flow behaviour of the fluid, whether it follows Newtonian flow or non-Newtonian flow, the Ostwald-de-Waele (OdW) model is employed using Equation (1) as discussed in introduction part of chapter 1 [3-5]. In this analysis, fitting of power law curves was applied to the shear stress vs. shear rate curve to calculate the values of consistency index (m) and power law index (n). The obtained values of m and n are displayed in Table 4.1.

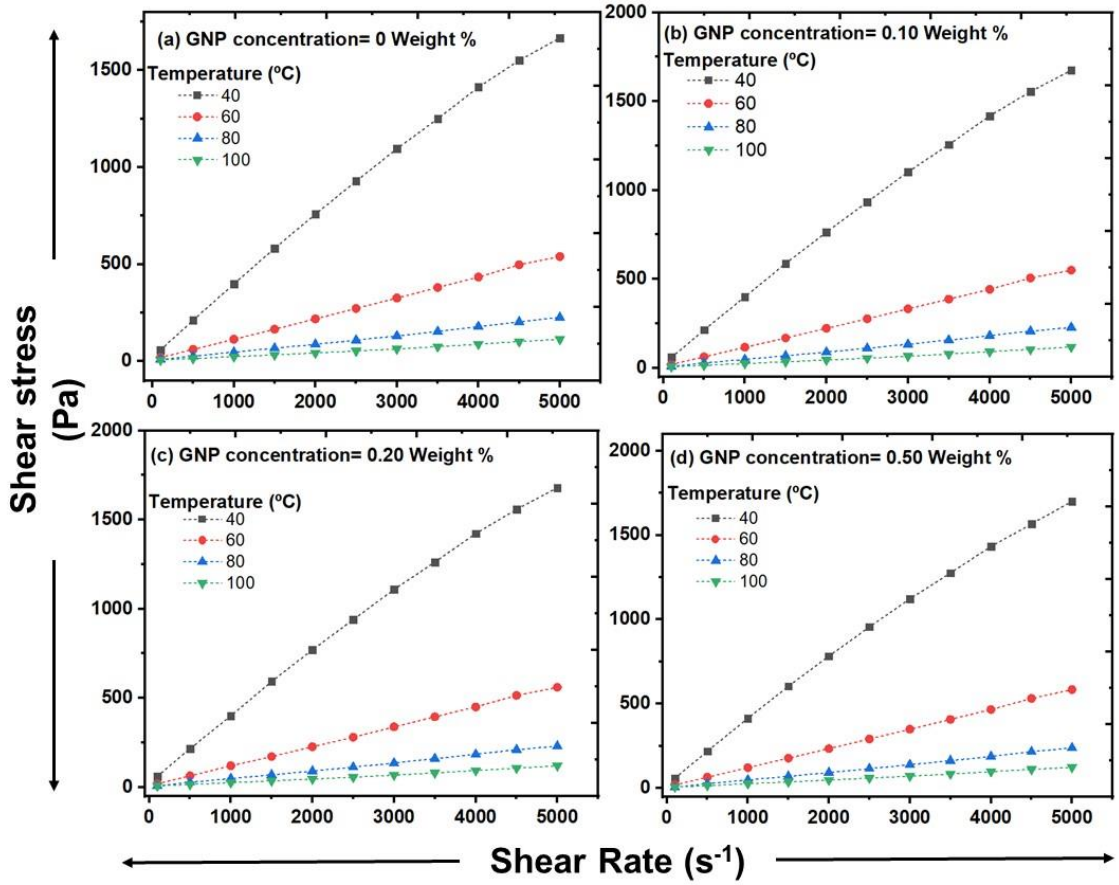

Fig. 4.20 (a-d): Shear stress vs. shear rate at various temperature for GNP/CO nanofluids.

As shown in Fig. 4.21, power law index (n) values are less than one at 40°C for all nano-additive GNP weight % and temperature ranges of the nanofluids, indicating a pseudo plastic non-Newtonian fluid flow behaviour. The values of n for all nano-additive GNP weight % and temperatures (60°C and 80°C) of the nanofluids are close to or equal to one, indicating a Newtonian fluid flow behaviour. For 100°C temperature, at lower concentration up to 0.2 weight %, CO and GNP/CO nanofluids show dilatant non-Newtonian fluid behaviour. While, at 0.5 weight %, GNP/CO nanofluid show mild

Newtonian fluid flow behaviour. This observation suggests that at higher temperature of 100°C, GNP/CO nanofluids shows different flow behaviours depending on nano-additive GNP. This may help in designing the GNP/CO nanofluid as per flow behaviour requirement in different industrial applications.

Table 4.3: The power law index (n) and consistency index (m) values of GNP/CO nano-fluids.

Temperature (°C)	Indexes	GNP concentration (Weight %)				
		0	**0.05**	**0.1**	**0.2**	**0.5**
40	m	959	972	985	1022	1118
	n	0.8780	0.8767	0.8753	0.8714	0.8617
60	m	123	125	127	131	130
	n	0.9850	0.9845	0.9839	0.9820	0.9871
80	m	40	41	43	44	42
	n	1.0125	1.0099	1.0074	1.0048	1.0151
100	m	17	17	17	19	27
	n	1.0349	1.0334	1.0319	1.0252	0.9905

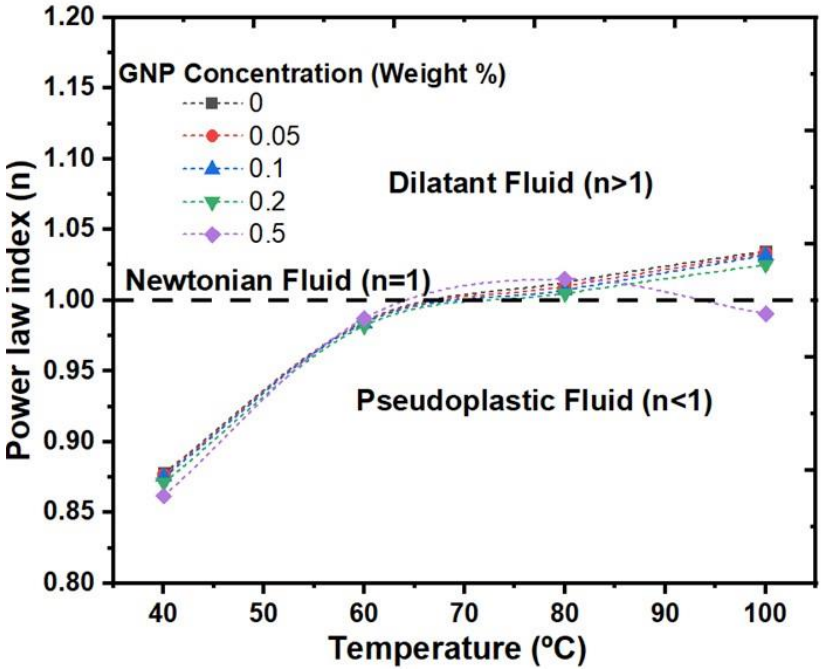

Fig. 4.21: Power law index for different solid mass fractions and temperature for GNP/CO nanofluids.

Furthermore, Fig. 4.22 depicts the relationship between the nanofluids' temperature & the consistency index (m) for different GNP weight concentrations. The data clearly demonstrate m value declines with increasing temperature. This indicates, as temperature rises, the fluid's mobility decreases, resulting in reduced flow resistance. It is noteworthy that the consistency index does not change much with the GNP concentration at higher

temperatures. This observation confirms that higher GNP concentrations in the base fluid do not substantially increase resistance to fluid flow.

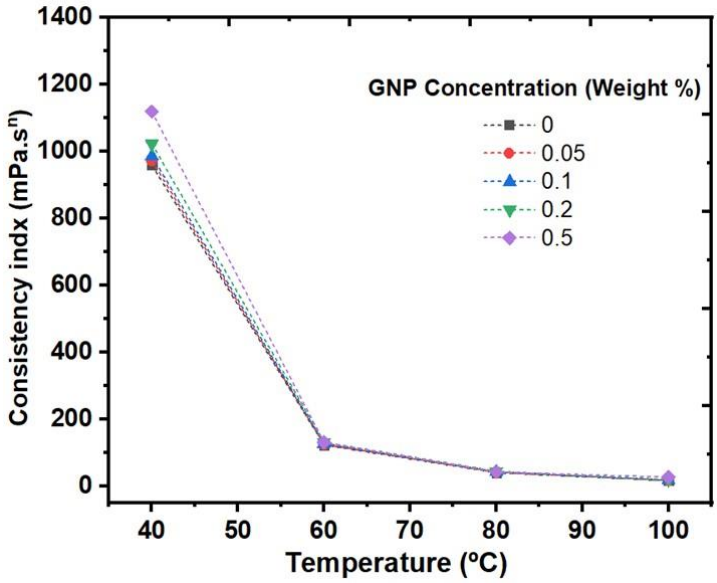

Fig. 4.22: Consistency index for different solid mass fractions and temperatures for GNP/CO nanofluids.

4.4.2: Thermal conductivity characteristics of GNP/CO nanofluids

In Fig. 4.23 (a), the thermal conductivity of pure CO and GNP/CO nanofluid is shown for GNP concentration over a temperature: 30°C to 70°C. The data reveal that thermal conductivity increases as increasing the GNP concentration. Moreover, at higher GNP concentrations, the thermal conductivity exhibits a steeper slope, indicating a more pronounced enhancement. This increase in thermal conductivity is attributed to the higher heat conductivity of GNP incorporated into the CO fluid. It is noteworthy to notice, thermal conductivity of both CO fluid and the GNP/CO nanofluid with a 0.05 weight % GNP concentration diminish as temperature increases. However, a reversal in thermal conductivity behaviour is observed at a GNP concentration above 0.1 weight % in the BO. In this case, the thermal conductivity of GNP/CO nanofluids increases with enhancing temperature. This is explained by the increased interaction and spread of GNP within the CO fluid at higher temperatures. These changes are driven by the energy transfer between the layers of the nanofluid, resulting in enhanced heat transfer capabilities of the nanofluids [6-8]. Overall, the findings show that GNP/CO nanofluids have enhanced thermal conductivity relative to the pure CO fluid.

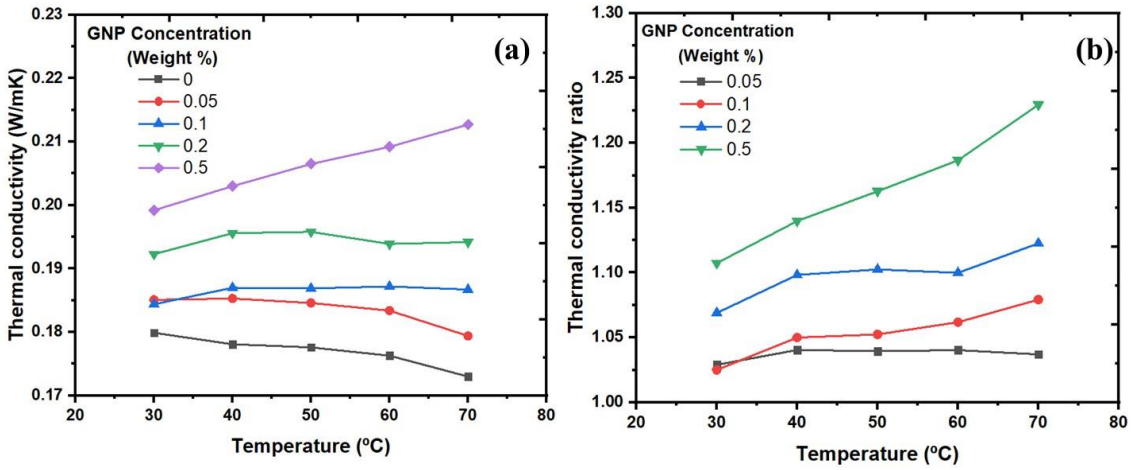

Fig. 4.23: (a) Thermal conductivity of GNP/CO nanofluids, and (b) thermal conductivity ratio of GNP/CO nanofluids.

The thermal conductivity ratio of the GNP/CO nanofluid relative to the CO base fluid is shown in Fig. 4.23 (b). The ratio increases with enhancing temperature. At low GNP weight %, there are minimal increases in thermal conductivity because of the lower concentration of GNP in the fluid. However, as the GNP concentration increases, the number of nanoparticles & their collisions also increases, resulting in effective heat transfer between the fluid layers [9, 10]. This results in greater thermal conductivity values for the GNP/CO nanofluid relative to the base CO fluid. In our study, the thermal conductivity of the GNP/CO nanofluid increased by 23% at 70°C for a GNP weight % of 0.5%. This significant enhancement demonstrates the capability of GNP/CO nanofluids to enhance heat transfer performance in diverse applications.

4.5: CO-based nanofluids containing MWCNT nano-additives (MWCNT/CO nanofluids)

In this study, a comprehensive rheological investigation was carried out to assess the dynamic viscosity of both pure CO and MWCNT/CO nanofluids under different MWCNT concentrations, shear rates, and temperature conditions. The main focus was to understand the influence of MWCNT weight % and temperature on the dynamic viscosity and thermal conductivity of MWCNT/CO nanofluids. The obtained results shed light on the potential uses of MWCNT/CO nanofluids as lubricating oils.

4.5.1: Flow characteristics of MWCNT/CO nanofluids using rheometry

Fig. 4.24 exhibits the impact of shear rate on the dynamic viscosity of MWCNT/CO nanofluids at different MWCNT weight% and temperatures: 40ºC to 100ºC. The findings indicated that the dynamic viscosity of both MWCNT/CO nanofluids and pure CO decreases linearly with increasing shear rates at 40ºC for all nano-additive concentrations. Notable observation found that at 40ºC temperature, as shear rate increases to maximum, all MWCNT/CO nanofluids exhibit nearly same dynamic viscosity indicating MWCNT nano-additive has not altered fluid characteristic at 40 ºC and high shear rate condition. At higher shear rates and higher temperatures i.e., 60ºC, 80ºC, and 100ºC, all fluids exhibit linear behaviour indicating Newtonian fluid characteristic i.e., fluids have a constant viscosity regardless of the shear rates applied. The experimental findings suggest a Newtonian fluid behaviour for both MWCNT/CO nanofluids and pure CO at higher shear rates and higher temperature within the experimental range. Furthermore, at higher shear rates and higher temperature, nanofluids with lower MWCNT weight % exhibit a slight shear-thinning behaviour compared to nanofluids with higher MWCNT weight %. This observation suggests that increased MWCNT concentration, represented by weight %, has a notable impact on maintaining Newtonian fluid behaviour in both MWCNT/CO nanofluids and pure CO.

Fig. 4.25 presents the influence of MWCNT weight % on the dynamic viscosity of constantly-temperatured nanofluids. The MWCNT concentration has a significant influence on the dynamic viscosity within the shear rate range of 100 to 5000 s^{-1}. At 40ºC dynamic viscosity of all nanofluids increases marginally with increasing MWCNT nano-additive concentration. However, rate of increase in dynamic viscosity with increasing

MWCNT nano-additive concentration became very less at all shear rates except 100 s^{-1}. Increased dynamic viscosity of nanofluids attributed to the increased flow resistancedepicted by the presence of solid MWCNT nano-additive in the CO fluid. Consequently, increasing the MWCNT nano-additive concentration results in higher nanofluid viscosity. However, it's important to note that the dynamic viscosity does not always increase significantly with concentration. For instance, in Fig. 4.4 (c) and 6(d), the increase in dynamic viscosity is relatively low compared to lower temperature of 40ºC.

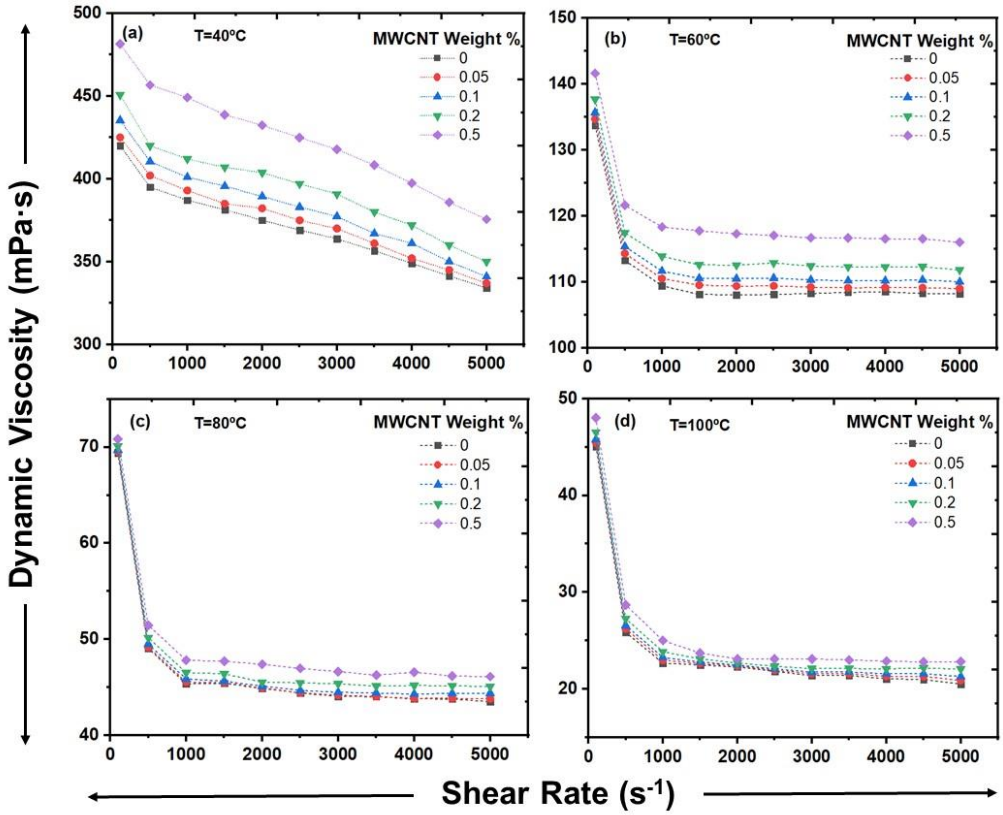

Fig. 4.24 (a-d): Effect of shear rate on dynamic viscosity of MWCNT/CO nanofluids at different mass fraction.

Fig. 4.26 depicts the influence of temperature on the dynamic viscosity of pure CO and MWCNT/CO nanofluids with varying nano-additive MWCNT weight %. This analysis is conducted at constant shear rates of 500 s^{-1} and 5000 s^{-1}. As the temperature rises from 40°C to 100°C, the dynamic viscosity drops for CO fluids and MWCNT/CO nanofluids. For instance, at a shear rate of 500 s^{-1}, the MWCNT/CO nanofluid with a 0.5 weight% MWCNT concentration shows a viscosity of 453 mPa at 40°C, which decreases to 29 mPa at 100°C. Similar trends are observed for other nano-additive MWCNT weight %. These observations can be attributed to a decreased intermolecular adhesion force as

temperature rises. Moreover, the effect of solid nano-additive MWCNT concentration on dynamic viscosity is more prominent at lower temperatures. However, this impact starts to diminish as the temperature increases.

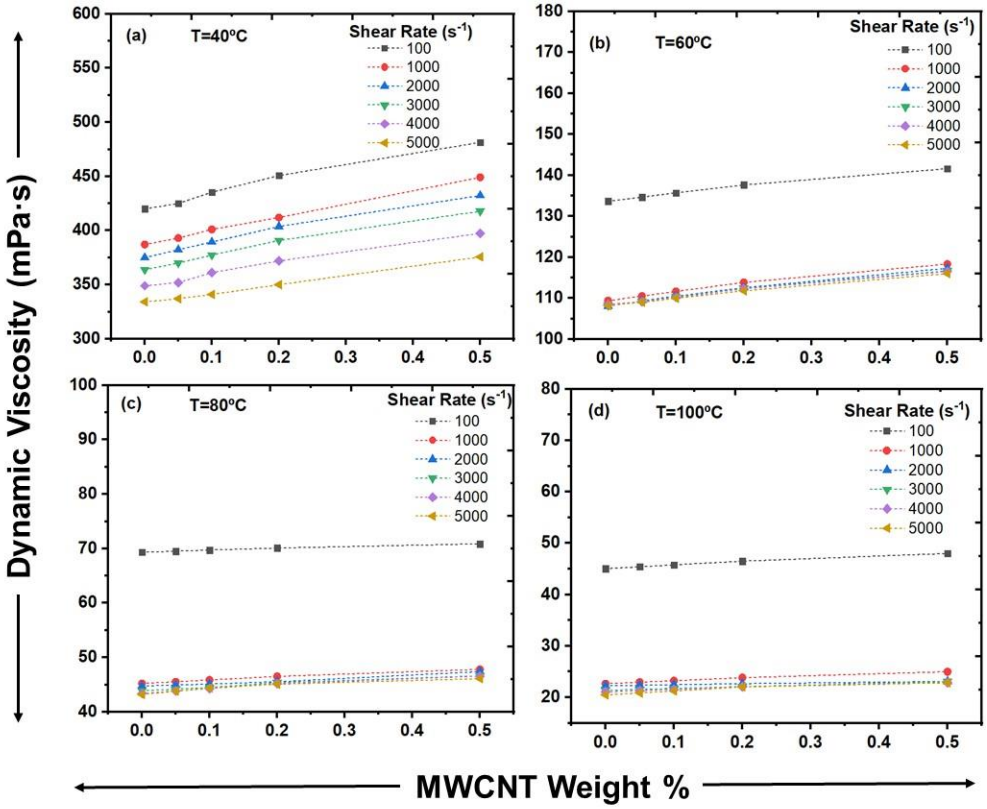

Fig. 4.25 (a-d): Effect of solid mass fractions on dynamic viscosity of MWCNT/CO nanofluids at different shear rates.

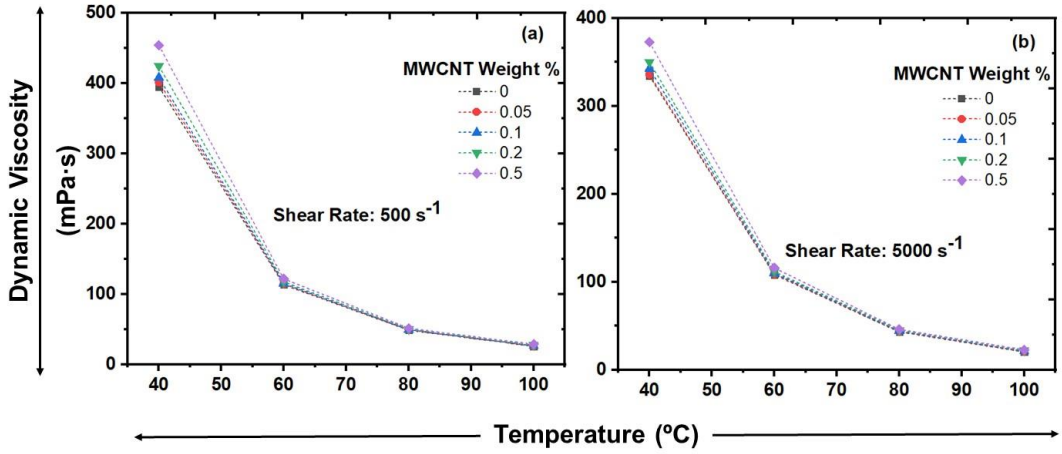

Fig. 4.26 (a-b): Effect of temperature on the dynamic viscosity of MWCNT/CO nanofluids at different solid mass fractions.

In Fig. 4.27 (a-d), the correlation between shear rate & shear stress of MWCNT/CO nanofluid is depicted at different temperatures for various MWCNT weight % (0.0, 0.05,

0.1, 0.2, and 0.5). The figures demonstrate that shear stress increases as shear rate increases across all temperatures. To determine the flow behaviour of the fluid, whether it follows Newtonian flow or non-Newtonian flow, the Ostwald-de-Waele (OdW) model is employed using Equation (1) as discussed in introduction part of chapter 1 [3-5]. In this analysis, fitting of power law curves was applied to the shear stress vs. shear rate curve to calculate the values of consistency index (m) and power law index (n). The obtained values of m and n are presented in Table 4.4.

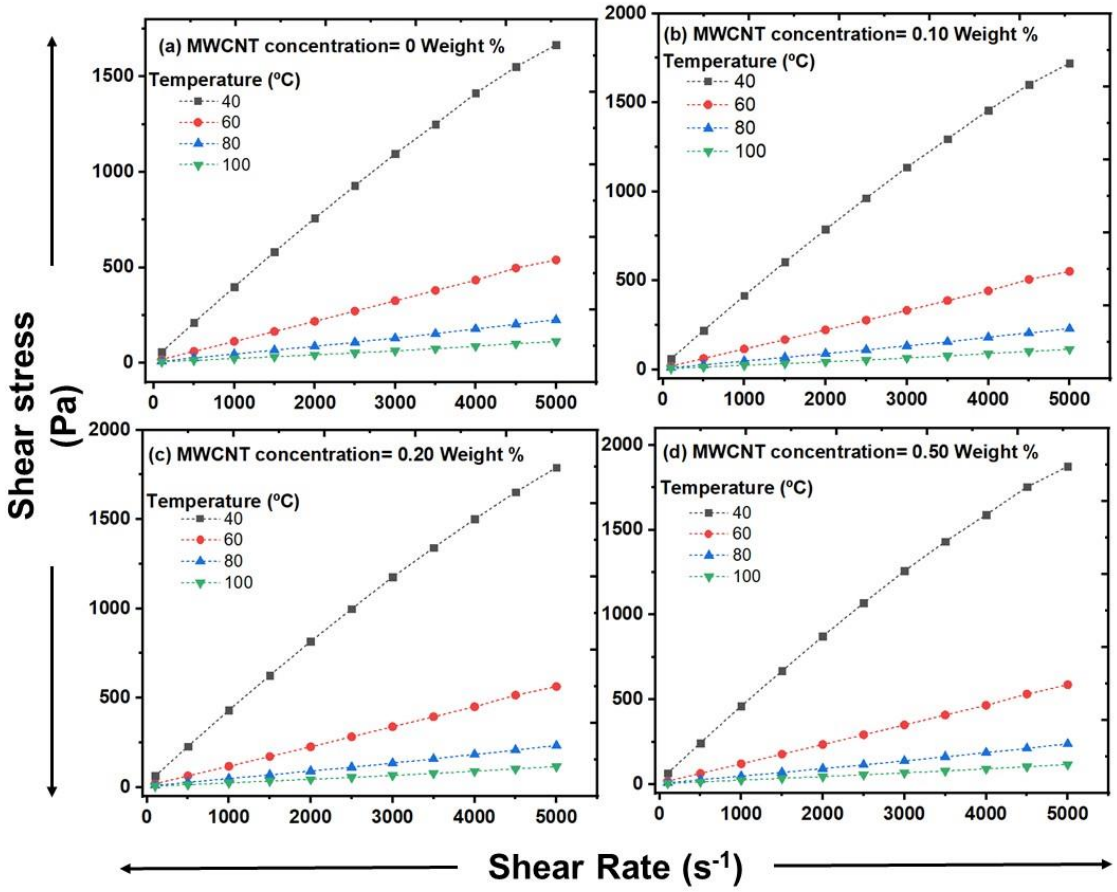

Fig. 4.27 (a-d): Shear stress vs. shear rate at various temperature for MWCNT/CO nanofluids.

As shown in Fig. 4.28, power law index (n) values are less than one at 40°C for all nano-additive MWCNT weight % and temperature ranges of the nanofluids, indicating a pseudo plastic non-Newtonian fluid flow behaviour. The values of n for all nano-additive MWCNT weight % and temperatures (60°C and 80°C) of the nanofluids are close to or equal to one, indicating a Newtonian fluid flow behaviour. For 100°C temperature, at lower concentration up to 0.1 weight %, CO and MWCNT/CO nanofluids show dilatant

non-Newtonian fluid behaviour. While, at 0.2 weight %, MWCNT/CO nanofluid show Newtonian fluid flow behaviour. Moreover, at 0.5 weight %, MWCNT/CO nanofluid show shift to pseudoplastic non-Newtonian fluid flow behaviour. This observation suggests that at higher temperature of 100°C, MWCNT/CO nanofluids shows different flow behaviours depending on nano-additive MWCNT concentrations. This may help in designing the MWCNT/CO nanofluid as per flow behaviour requirement in different industrial applications.

Table 4.4: The power law index (n) and consistency index (m) values of MWCNT/CO nano-fluids.

Temperature (°C)	Indexes	MWCNT concentration (Weight %)				
		0	**0.05**	**0.1**	**0.2**	**0.5**
40	m	959	949	1036	1077	1308
	n	0.8780	0.8819	0.8726	0.8721	0.8557
60	m	123	123	124	125	129
	n	0.9850	0.9868	0.9864	0.9877	0.9885
80	m	40	41	42	43	47
	n	1.0125	1.0101	1.0097	1.0070	1.0007
100	m	17	17	18	22	29
	n	1.0349	1.0300	1.0236	1.0050	0.9717

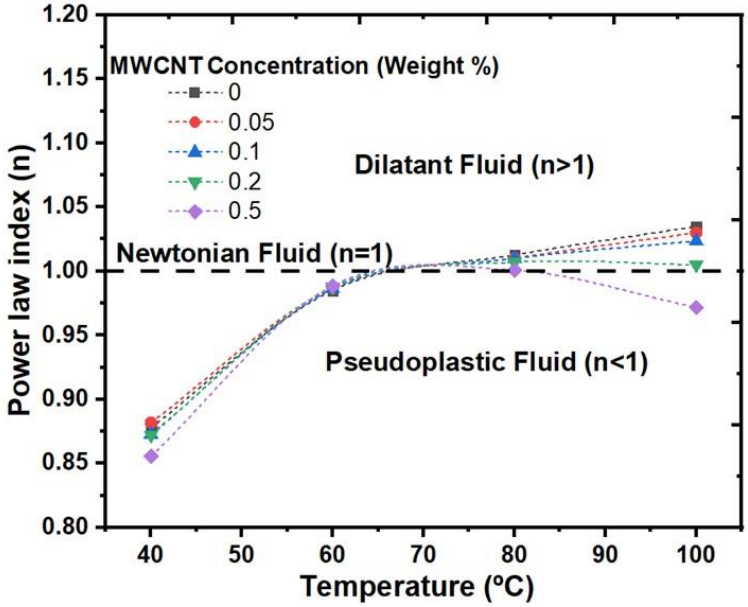

Fig. 4.28: Power law index for different solid mass fractions and temperature for MWCNT/CO nanofluids.

Furthermore, Fig. 4.29 depicts the relationship between the nanofluids' temperature & the consistency index (m) for different MWCNT weight concentrations. The results clearly demonstrate m value declines with increasing temperature. This indicates, as

temperature rises, the fluid's mobility decreases, resulting in reduced flow resistance. It is noteworthy that the consistency index does not change much with the MWCNT concentration at higher temperatures. This observation confirms that higher MWCNT concentrations in the base fluid do not substantially increase resistance to fluid flow.

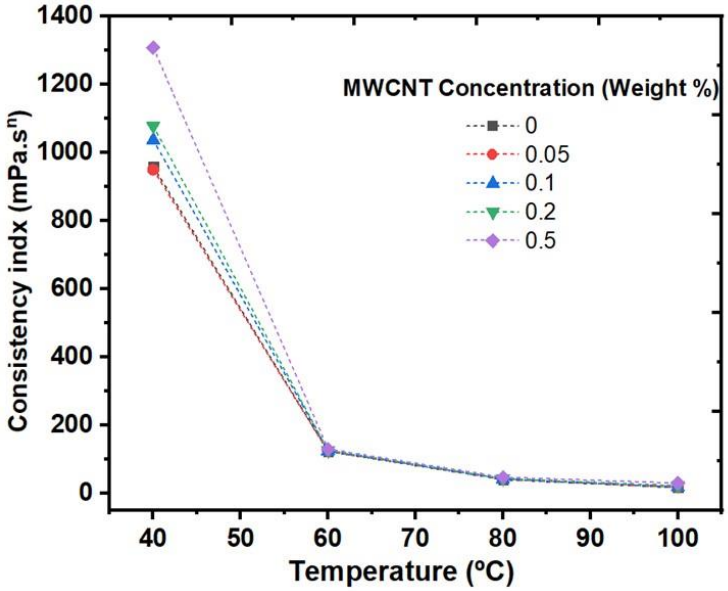

Fig. 4.29: Consistency index for different solid mass fractions and temperatures for MWCNT/CO nanofluids.

4.5.2: Thermal conductivity characteristics of MWCNT/CO nanofluids

In Fig. 4.30 (a), the thermal conductivity of pure CO and MWCNT/CO nanofluid is shown for MWCNT concentration over a temperature: 30°C to 70°C. The data reveal that thermal conductivity increases as increasing the MWCNT concentration. Moreover, at higher MWCNT concentrations, the thermal conductivity exhibits a steeper slope, indicating a more pronounced enhancement. This increase in thermal conductivity is attributed to the higher heat conductivity of MWCNT incorporated into the CO fluid. It is noteworthy to notice, thermal conductivity of both CO fluid and the MWCNT/CO nanofluid with a 0.05 weight % MWCNT concentration diminish as temperature increases. However, a reversal in thermal conductivity behaviour is observed at a MWCNT concentration above 0.1 weight % in the BO. In this case, the thermal conductivity of MWCNT/CO nanofluids increases with enhancing temperature. This is explained by the increased interaction and spread of MWCNT within the CO fluid at higher temperatures. These changes are driven by the energy transfer between the layers of the nanofluid, resulting in enhanced heat transfer capabilities of the nanofluids [6-8]. Overall, the findings

show that MWCNT/CO nanofluids have enhanced thermal conductivity relative to the pure CO fluid.

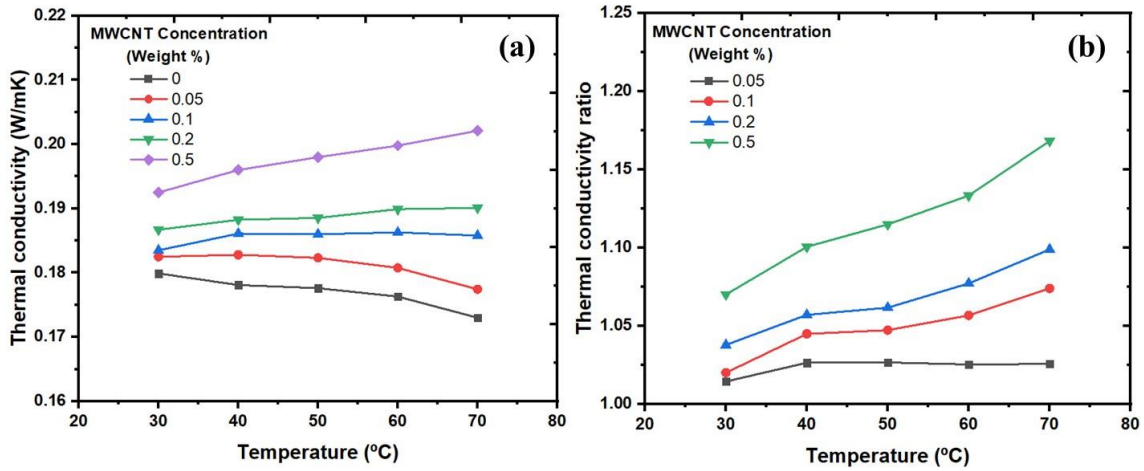

Fig. 4.30: (a) Thermal conductivity of MWCNT/CO nanofluids, and (b) thermal conductivity ratio of MWCNT/CO nanofluids.

The thermal conductivity ratio of the MWCNT/CO nanofluid relative to the CO base fluid is shown in Fig. 4.30 (b). The ratio increases with enhancing temperature. At low MWCNT weight %, there are minimal increases in thermal conductivity because of the lower concentration of MWCNT in the fluid. However, as the MWCNT concentration increases, the number of nanoparticles & their collisions also increases, resulting in effective heat transfer between the fluid layers [9, 10]. This results in greater thermal conductivity values for the MWCNT/CO nanofluid relative to the base CO fluid. In our study, the thermal conductivity of the MWCNT/CO nanofluid increased by 16.8% at 70°C for a MWCNT weight % of 0.5%. This significant enhancement demonstrates the capability of MWCNT/CO nanofluids to enhance heat transfer performance in diverse applications.

4.6: Results and discussion

To assess the enhancement in the flow and thermal conductivity properties of the CO dispersed with different nano-additives (Al_2O_3, ZnO, GNP, and MWCNT), a series of analysis were performed. The overall observations found through the experiments were furnished below.

As per the Ostwald-de-Waele (OdW) model, pure CO and CO-based nanofluids with different nano-additives were evaluated for determining the fluid flow characteristics under various shear stress, temperatures and nano-additives concentration conditions [3-5]. All CO and CO-based nanofluids flow behaviour are represented in Table 4.5.

All the CO-based nanofluids exhibit pseudoplastic non-Newtonian fluid flow characteristic at 40°C which indicates fluids viscosity, or the flow resistance, decreases as the force or shear rate increases. In other words, the more you stir or squeeze, the easier it flows. However, if you stop applying the force, it thickens up again over the time [11-13]. All the CO and CO-based nanofluids exhibits Newtonian fluid flow behaviour except CO-ZnO nanofluid of 0.2 and 0.5 weight %. Newtonian fluids exhibit a constant viscosity regardless of the amount of force applied to them. This behaviour is described by Newton's law of viscosity, which states that the shear stress (force per unit area) within the fluid is directly proportional to the velocity gradient (rate of change of velocity with respect to distance) in the direction perpendicular to the force applied [14]. In essence, shear rate & shear stress in Newtonian fluids are correlated linearly, meaning if you double the force applied, you double the rate of flow [15]. The CO exhibit dilatant non-Newtonian fluid characteristics at 100°C. Dilatant fluids become thicker and more viscous under stress [16]. The name "dilatant" comes from the fact that these fluids dilate or expand when force is applied, causing them to resist flow more strongly. This behaviour is often described as "shear thickening" because the viscosity increases as shear rate applied increases [17-19]. As shown in Table 4.5, the CO-based nanofluids exhibits various fluid flow behaviour at 100°C depending on nature of nano-additives.

Pure CO and CO-based nanofluids with different nano-additives were evaluated for determining the thermal conductivity characteristics under different temperature and nano-additives concentration conditions. The thermal conductivity enhancement of nanofluids in percentage in compared to pure CO at temperature is shown in Table 4.6. Carbon based nano-additives (GNP and MWCNT) increases thermal conductivity of base fluid greater

than the metal-oxide based nano-additives (Al_2O_3 and ZnO) [20]. GNP nano-additive shows maximum thermal conductivity enhancement of 23% at 0.5 weight % concentration at 70°C. GNP and MWCNT at 0.5 weight % nano-additives concentration, increases thermal conductivity of base CO fluid by more than 10% for all temperature range measured.

Table 4.5: Flow behaviour of CO-based nanofluids.

Nanofluid	Nano-additive weight %	Temperature (°C)			
		40	60	80	100
CO	Pure	PP	N	N	D
Al_2O_3/CO	0.05	PP	N	N	D
	0.1	PP	N	N	N
	0.2	PP	N	N	N
	0.5	PP	N	N	PP
ZnO/CO	0.05	PP	N	N	D
	0.1	PP	N	N	D
	0.2	PP	PP	N	N
	0.5	PP	PP	N	N
GNP/CO	0.05	PP	N	N	D
	0.1	PP	N	N	D
	0.2	PP	N	N	D
	0.5	PP	N	N	N
MWCNT/CO	0.05	PP	N	N	D
	0.1	PP	N	N	D
	0.2	PP	N	N	N
	0.5	PP	N	N	PP

PP: Pseudo plastic non-Newtonian fluid, D: Dilatant non-Newtonian fluid, N: Newtonian fluid

GNP and MWCNT exhibit higher thermal conductivity compared to metal-oxide nano-additives due to their unique structural and material properties. Graphene is a two-dimensional material composed of a single layer of carbon atoms arranged in a hexagonal lattice, while carbon nanotubes are cylindrical structures made of rolled-up graphene sheets. These carbon-based nanomaterials possess excellent thermal conductivity because of their highly ordered atomic structures and strong covalent bonding between carbon

atoms. This allows them to efficiently transfer heat through phonon vibrations along their carbon-carbon bonds. Additionally, carbon-based nanomaterials like GNP and MWCNT have higher aspect ratios and larger surface areas, which facilitate better dispersion and interaction within the fluid. This enhanced dispersion allows for more effective thermal conduction pathways throughout the fluid, further increasing its overall thermal conductivity [21, 22]. In contrast, metal-oxide nano-additives (Al_2O_3 and ZnO) typically have lower thermal conductivity because of their crystalline structures and the presence of lattice defects, grain boundaries, and phonon scattering sites. These factors hinder the efficient transfer of heat through the material, resulting in lower thermal conductivity compared to carbon-based nanomaterials [7, 23, 24].

Table 4.6: Enhancement of thermal conductivity (%) of CO-based nanofluids**.**

Nanofluid	**Nano-additive weight %**	**Temperature (°C)**				
		30	**40**	**50**	**60**	**70**
Al_2O_3/CO	0.05	0.7	1.9	1.6	1.9	2.9
	0.1	1.5	2.9	3.6	4.7	6.9
	0.2	2.3	4.2	4.7	6.1	9.5
	0.5	4.7	7.2	8.8	**12.2**	**16.2**
ZnO/CO	0.05	0.3	1.7	1.9	1.3	1.2
	0.1	0.7	3.1	3.4	4.3	6.0
	0.2	1.8	3.9	4.7	5.8	8.1
	0.5	2.6	5.3	7.5	9.5	**13.9**
GNP/CO	0.05	2.9	4.0	3.9	4.0	**3.7**
	0.1	2.5	5.0	5.2	6.2	**7.9**
	0.2	6.9	9.8	**10.2**	**10.0**	**12.3**
	0.5	**10.7**	**14.0**	**16.3**	**18.7**	**22.9**
MWCNT/CO	0.05	1.4	2.6	2.7	2.5	2.6
	0.1	2.0	4.5	4.7	5.7	7.4
	0.2	3.8	5.7	6.2	7.7	9.9
	0.5	7.0	**10.1**	**11.5**	**13.3**	**16.8**

In metal-oxide nano-additives, Al_2O_3 nano-additive exhibits better thermal conductivity enhancement compared to ZnO nano-additive. Al_2O_3 nano-additive has a higher thermal conductivity intrinsic to its crystal structure compared to ZnO nano-

additive. Al_2O_3 nano-additive possesses a higher thermal conductivity because of its dense crystalline structure and strong atomic bonding, which allows heat to propagate more efficiently through the material.

Overall, the unique structural and material properties of GNP and MWCNT contribute to their superior ability to enhance the thermal conductivity of fluids compared to metal-oxide nano-additives (Al_2O_3 and ZnO).

4.7: Chapter Conclusion

The present study investigates the stability and flow behaviour of CO-based nanofluids with different nano-additive concentrations at 0.05, 0.1, 0.2, and 0.5 weight %. Using versatile ultrasonically-assisted technique, the Al_2O_3/CO, ZnO/CO, GNP/CO and MWCNT/CO nanofluids were successfully stabilized. Rheological investigations were carried out at various shear rates and temperatures, revealing a different flow behaviour across all samples. The study contributes to the existing knowledge on thermophysical properties of CO and sets the stage for further advancements in the field. The following are the key investigations of the study:

1. The dynamic viscosity of both the CO fluid and CO-based nanofluids exhibited a reduction at the initial increase in shear rate of 100 s^{-1} and at temperature 40°C. Furthermore, the viscosity remained stable as the shear rate and temperature was further increased across all temperatures studied.
2. With increasing temperature from 40°C to 100°C, the dynamic viscosity of all nanofluids decreases across all nano-additives concentrations. At lower temperatures of 40ºC, the nano-additives weight% and type of nano-additives have a significant impact on viscosity, while its influence diminishes as the temperature rises.
3. The power law index (n) values for 0.5 weight % GNP/CO nanofluids, obtained at 60°C, 80°C and 100°C temperature ranges, are close to or equal to 1. This observation confirms the Newtonian flow behaviour of GNP/CO nanofluids. The power law index (n) values for 0.2 weight % Al_2O_3/CO and MWCNT/CO nanofluids, obtained at 60°C, 80°C and 100°C temperature ranges, are close to or equal to 1 that confirms the Newtonian flow behaviour of Al_2O_3/CO and MWCNT/CO nanofluids. The ZnO/CO nanofluids shows instability in flow behaviour as nano-additive concentration and temperature changes.
4. The concentration of nano-additives significantly influences the dynamic viscosity and thermal conductivity behaviour of CO-based nanofluids. The interactions between nano-additives and CO play a crucial role in enhancing the heat conduction and transfer capabilities of CO-based nanofluids relative to the base CO fluid. In fact, the thermal conductivity was observed to increase by 23% in the best-case scenario at 70ºC for a GNP/CO nanofluid with a weight % of 0.5%. Carbon based nano-additives

GNP and MWCNT have higher impact on increasing thermal conductivity of base CO fluid as compared to metal oxide-based nano-additives i.e., Al_2O_3 and ZnO.

5. For consistent lubrication in engine components applications where Newtonian fluid with high thermal conductivity is desirable, 0.5 weight % GNP/CO nanofluid is suitable nanofluid.
6. Pseudoplastic fluids like grease, adjust viscosity under shear stress, providing both lubrication and sealing properties, ideal for high-pressure and temperature environments within applied engines. For such applications, 0.5 weight % Al_2O_3/CO and MWCNT/CO are suitable nanofluids with approximate 17% thermal conductivity improvement as compared to CO base fluid.
7. Dilatant fluids, like some specialized additives, offer shear thickening properties, enhancing lubricant performance under extreme conditions by forming protective layers. Engine oils formulated with a blend of these fluid behaviours cater to diverse operational demands, ensuring efficient lubrication, friction reduction, and component protection, contributing to optimal engine performance and longevity in various applications. 0.2 weight % GNP/CO is suitable nanofluids with approximate 12% thermal conductivity improvement as compared to CO base fluid at higher temperature.

The results of our investigation clearly indicate that GNP/CO nanofluids hold substantial promise as valuable and cost-effective materials for diverse lubrication and heat transfer applications. However, we recognize the need for further exploration and meticulous calculations of heat transfer coefficients in practical heat transfer contexts. This approach will provide a comprehensive evaluation of their real-world efficacy.

4.8: References

[1] Mubofu, Egid B, Castor oil as a potential renewable resource for the production of functional materials, Sustainable Chemical Processes, 4 (2016) 1-12.

[2] McKeon, Thomas A. Castor (Ricinus communis L.), Industrial oil crops, AOCS Press, (2016) 75-112.

[3] Afrand, Masoud, Davood Toghraie, and Behrooz Ruhani, Effects of temperature and nano-additives concentration on rheological behavior of Fe_3O_4–Ag/EG hybrid nanofluid: an experimental study, Experimental Thermal and Fluid Science, 77 (2016) 38-44.

[4] Bharath, Bhavin K., and V. Arul Mozhi Selvan, An experimental investigation on rheological and heat transfer performance of hybrid nanolubricant and its effect on the vibration and noise characteristics of an automotive spark-ignition engine, International Journal of Thermophysics, 42 (2021) 1-30.

[5] Vora, Vishal, Rakesh K. Sharma, and D. P. Bharambe, Investigation of rheological and thermal conductivity properties of castor oil nanofluids containing graphene nanoplatelets, International Journal of Thermophysics, 44.10 (2023) 155.

[6] Godson, Lazarus, B. Raja, D. Mohan Lal, and S. E. A. Wongwises, Enhancement of heat transfer using nanofluids-an overview, Renewable and sustainable energy reviews, 14 (2010) 629-641.

[7] Lenin, Ramanujam, Pattayil Alias Joy, and Chandan Bera, A review of the recent progress on thermal conductivity of nanofluid, Journal of Molecular Liquids, 338 (2021) 116929.

[8] Machrafi, Hatim, and Georgy Lebon, The role of several heat transfer mechanisms on the enhancement of thermal conductivity in nanofluids, Continuum Mechanics and Thermodynamics, 28 (2016) 1461-1475.

[9] Kakaç, Sadik, and Anchasa Pramuanjaroenkij, Review of convective heat transfer enhancement with nanofluids, International journal of heat and mass transfer, 52 (2009): 3187-3196.

[10] Amani, Mohammad, Pouria Amani, Mehdi Bahiraei, Mohammad Ghalambaz, Goodarz Ahmadi, Lian-Ping Wang, Somchai Wongwises, and Omid Mahian, Latest developments in nanofluid flow and heat transfer between parallel surfaces: A critical review, Advances in Colloid and Interface Science, 294 (2021) 102450.

[11] Cross, Malcolm M, Rheology of non-Newtonian fluids: a new flow equation for pseudoplastic systems, Journal of colloid science, 20 (1965): 417-437.

[12] Guedda, M., and R. Kersner, Non-Newtonian pseudoplastic fluids: Analytical results and exact solutions, International Journal of Non-Linear Mechanics, 46 (2011) 949-957.

[13] Liu, Shengna, Xuehui Chen, and Liancun Zheng, Heat transfer of pseudo-plastic fluid in shear flow with field correlation, Journal of the Taiwan Institute of Chemical Engineers, 146 (2023) 104874.

[14] Walters, K. and W.M. Jones, 2 - Measurement of viscosity, in Instrumentation Reference Book (Third Edition), W. Boyes, Editor, Butterworth-Heinemann: Burlington, (2003) 45-52.

[15] Kragh, A. M., Viscosity, Determination of the size and shape of protein molecules, Pergamon, (1961) 173-209.

[16] Nakanishi, Hiizu, Shin-Ichiro Nagahiro, and Namiko Mitarai, Colloidal dispersions, suspensions, and aggregates-Fluid dynamics of dilatant fluids (11 pages) 011401, Physical Review-Section E-Statistical Nonlinear and Soft Matter Physics, 85 (2012).

[17] Boersma, Willem H., Jozua Laven, and Hans N. Stein, Shear thickening (dilatancy) in concentrated dispersions, AIChE journal, 36 (1990) 321-332.

[18] Vasu, Buddakkagari, Rama Subba Reddy Gorla, P. V. S. N. Murthy, and O. Anwar Bég, Entropy analysis of a convective film flow of a power-law fluid with nanoparticles along an inclined plate, Journal of Applied Mechanics and Technical Physics, 60 (2019) 827-841.

[19] Griskey, Richard G., and Richard G. Green, Flow of dilatant (shear-thickening) fluids, AIChE Journal, 17 (1971) 725-728.

[20] Rajamony, R.K., Paw, J.K.S., Pandey, A.K., Tak, Y.C., Pasupuleti, J., Tiong, S.K., Yusaf, T., Samykano, M., Sofiah, A.G.N., Kalidasan, B. and Ahmed, O.A., Energizing the thermophysical properties of phase change material using carbon-based nano additives for sustainable thermal energy storage application in photovoltaic thermal systems, Materials Today Sustainability, 25 (2024) 100658.

[21] Younes, Hammad, Mingyang Mao, SM Sohel Murshed, Ding Lou, Haiping Hong, and G. P. Peterson, Nanofluids: Key parameters to enhance thermal conductivity and its applications, Applied Thermal Engineering, 207 (2022) 118202.

[22] Jebasingh, B. Eanest, and A. Valan Arasu, A comprehensive review on latent heat and thermal conductivity of nanoparticle dispersed phase change material for low-temperature applications, Energy Storage Materials, 24 (2020) 52-74.

[23] Wanatasanapan, V. Vicki, M. Z. Abdullah, and P. Gunnasegaran, Effect of TiO_2-Al_2O_3 nanoparticle mixing ratio on the thermal conductivity, rheological properties, and dynamic viscosity of water-based hybrid nanofluid, Journal of Materials Research and Technology, 9 (2020) 13781-13792.

[24] Apmann, Kevin, Ryan Fulmer, Alberto Soto, and Saeid Vafaei, Thermal conductivity and viscosity: Review and optimization of effects of nanoparticles, Materials, 14 (2021) 1291.